



Charged-particle distributions in root s=13 TeV pp interactions measured with the ATLAS detector at the LHC

Aad, G.; Abbott, B.; Abdallah, J.; Abdinov, O.; Abeloos, B.; Aben, R.; Abolins, M.; AbouZeid, O.S.; Nitzan, Abraham; Abramowicz, H.; Dam, Mogens; Hansen, Jørn Dines; Hansen, Jørgen Beck; Hansen, Peter Henrik; Pingel, Almut Maria; Petersen, Troels Christian; Thomsen, Lotte Ansgaard; Alonso Diaz, Alejandro; Monk, James William; Galster, Gorm Aske Gram Krohn; Xella, Stefania; Løvschall-Jensen, Ask Emil; Wiglesworth, Graig; Pedersen, Lars Egholm; Pingel, Almut Maria

Published in:
Physics Letters B

DOI:
[10.1016/j.physletb.2016.04.050](https://doi.org/10.1016/j.physletb.2016.04.050)

Publication date:
2016

Document version
Publisher's PDF, also known as Version of record

Document license:
[CC BY](#)

Citation for published version (APA):
Aad, G., Abbott, B., Abdallah, J., Abdinov, O., Abeloos, B., Aben, R., Abolins, M., AbouZeid, O. S., Nitzan, A., Abramowicz, H., Dam, M., Hansen, J. D., Hansen, J. B., Hansen, P. H., Pingel, A. M., Petersen, T. C., Thomsen, L. A., Alonso Diaz, A., Monk, J. W., ... Pingel, A. M. (2016). Charged-particle distributions in root s=13 TeV pp interactions measured with the ATLAS detector at the LHC. *Physics Letters B*, 758, 67-88.
<https://doi.org/10.1016/j.physletb.2016.04.050>



Charged-particle distributions in $\sqrt{s} = 13$ TeV pp interactions measured with the ATLAS detector at the LHC

ATLAS Collaboration^{*}

ARTICLE INFO

Article history:

Received 5 February 2016

Received in revised form 11 April 2016

Accepted 25 April 2016

Available online 27 April 2016

Editor: H. Weerts

ABSTRACT

Charged-particle distributions are measured in proton–proton collisions at a centre-of-mass energy of 13 TeV, using a data sample of nearly 9 million events, corresponding to an integrated luminosity of $170 \mu\text{b}^{-1}$, recorded by the ATLAS detector during a special Large Hadron Collider fill. The charged-particle multiplicity, its dependence on transverse momentum and pseudorapidity and the dependence of the mean transverse momentum on the charged-particle multiplicity are presented. The measurements are performed with charged particles with transverse momentum greater than 500 MeV and absolute pseudorapidity less than 2.5, in events with at least one charged particle satisfying these kinematic requirements. Additional measurements in a reduced phase space with absolute pseudorapidity less than 0.8 are also presented, in order to compare with other experiments. The results are corrected for detector effects, presented as particle-level distributions and are compared to the predictions of various Monte Carlo event generators.

© 2016 CERN for the benefit of the ATLAS Collaboration. Published by Elsevier B.V. This is an open access article under the CC BY license (<http://creativecommons.org/licenses/by/4.0/>). Funded by SCOAP³.

1. Introduction

Charged-particle measurements in proton–proton (pp) collisions provide insight into the strong interaction in the low-energy, non-perturbative region of quantum chromodynamics (QCD). Particle interactions at these energy scales are typically described by QCD-inspired models implemented in Monte Carlo (MC) event generators with free parameters that can be constrained by such measurements. An accurate description of low-energy strong interaction processes is essential for simulating single pp interactions as well as the effects of multiple pp interactions at high instantaneous luminosity in hadron colliders. Charged-particle distributions have been measured previously in pp and proton–antiproton collisions at various centre-of-mass energies [1–7] (and references therein).

This paper presents inclusive measurements of primary charged-particle distributions in pp collisions at a centre-of-mass energy of $\sqrt{s} = 13$ TeV, using data recorded by the ATLAS experiment [8] at the Large Hadron Collider (LHC) corresponding to an integrated luminosity of approximately $170 \mu\text{b}^{-1}$. Here inclusive means that all processes in pp interactions are included and no attempt to correct for certain types of process, such as diffraction, is made. These measurements, together with previous results, shed light on the evolution of charged-particle multiplicities with centre-of-

mass energy, which is poorly constrained. A strategy similar to that in Ref. [1] is used, where more details of the analysis techniques are given. The distributions are measured using tracks from primary charged particles, corrected for detector effects, and are presented as inclusive distributions in a well-defined kinematic region. Primary charged particles are defined as charged particles with a mean lifetime $\tau > 300$ ps, either directly produced in pp interactions or from subsequent decays of directly produced particles with $\tau < 30$ ps; particles produced from decays of particles with $\tau > 30$ ps, called secondary particles, are excluded. This definition differs from earlier analyses in that charged particles with a mean lifetime $30 < \tau < 300$ ps were previously included. These are charged strange baryons and have been removed due to the low efficiency of reconstructing them.¹ All primary charged particles are required to have a momentum component transverse to the beam direction,² p_T , of at least 500 MeV and absolute pseudorapidity, $|\eta|$, less than 2.5. Each event is required to have at least one primary charged particle.

¹ Since strange baryons tend to decay within the detector volume, especially if they have low momentum, they often do not leave enough hits to reconstruct a track, leading to a track reconstruction efficiency of approximately 0.3%.

² ATLAS uses a right-handed coordinate system with its origin at the nominal interaction point (IP) in the centre of the detector and the z -axis along the beam pipe. The x -axis points from the IP to the centre of the LHC ring, and the y -axis points upward. Cylindrical coordinates (r, ϕ) are used in the transverse plane, ϕ being the azimuthal angle around the beam pipe. The pseudorapidity is defined in terms of the polar angle θ as $\eta = -\ln \tan(\theta/2)$.

^{*} E-mail address: atlas.publications@cern.ch.

In these events the following distributions are measured:

$$\frac{1}{N_{\text{ev}}} \cdot \frac{dN_{\text{ch}}}{d\eta}, \quad \frac{1}{N_{\text{ev}}} \cdot \frac{1}{2\pi p_T} \cdot \frac{d^2N_{\text{ch}}}{d\eta dp_T}, \quad \text{and} \quad \frac{1}{N_{\text{ev}}} \cdot \frac{dN_{\text{ev}}}{dn_{\text{ch}}}$$

as well as the mean p_T ($\langle p_T \rangle$) of all primary charged particles versus n_{ch} . Here n_{ch} is the number of primary charged particles in an event, N_{ev} is the number of events with $n_{\text{ch}} \geq 1$, and N_{ch} is the total number of primary charged particles in the data sample.³ The measurements are also presented in a phase space that is common to the ATLAS, CMS [9] and ALICE [10] detectors in order to ease comparison between experiments. For this purpose an additional requirement of $|\eta| < 0.8$ is made for all primary charged particles. These results are presented in Appendix A. Finally, the mean number of primary charged particles for $\eta = 0$ is compared to previous measurements at different centre-of-mass energies. The measurements are compared to particle-level MC predictions.

The remainder of this paper is laid out as follows. The relevant components of the ATLAS detector are described in Section 2. The MC event generators and detector simulation used in the analysis are introduced in Section 3. The selection criteria applied to the data and the contributions from background events are discussed in Sections 4 and 5 respectively. The selection efficiency and corresponding corrections to the data are discussed in Sections 6 and 7 respectively. The corrected results are compared to theoretical predictions in Section 8 and a conclusion is given in Section 9. The measurement of primary charged particles in the reduced phase space of $|\eta| < 0.8$ is presented in Appendix A.

2. ATLAS detector

The ATLAS detector covers almost the whole solid angle around the collision point with layers of tracking detectors, calorimeters and muon chambers. For the measurements presented in this paper, the tracking devices and the trigger system are of particular importance.

The inner detector (ID) has full coverage in ϕ and covers the pseudorapidity range $|\eta| < 2.5$. It consists of a silicon pixel detector (pixel), a silicon microstrip detector (SCT) and a transition radiation straw-tube tracker (TRT). These detectors span a sensitive radial distance from the interaction point of 33–150 mm, 299–560 mm and 563–1066 mm respectively, and are situated inside a solenoid that provides a 2 T axial magnetic field. The barrel (each end-cap) consists of four (three) pixel layers, four (nine) double-layers of single-sided silicon microstrips with a 40 mrad stereo angle between the inner and outer part of a double-layer, and 73 (160) layers of TRT straws. The innermost pixel layer, the insertable B-layer (IBL) [11], was added between Run 1 and Run 2 of the LHC, around a new narrower (radius of 25 mm) and thinner beam pipe. It is composed of 14 lightweight staves arranged in a cylindrical geometry, each made of 12 silicon planar sensors in its central region and 2×4 3D sensors at the ends. The IBL pixel dimensions are $50 \times 250 \mu\text{m}^2$ in the ϕ and z directions (compared with $50 \times 400 \mu\text{m}^2$ for other pixel layers). The smaller radius and the reduced pixel size result in improvements of both the transverse and longitudinal impact parameter resolutions. In addition, new services have been implemented which significantly reduce the material at the boundaries of the active tracking volume. A track from a charged particle traversing the barrel detector typically has 12 silicon measurement points (hits), of which four are pixel and eight SCT, and more than 30 TRT straw hits.

³ The factor $2\pi p_T$ in the p_T spectrum comes from the Lorentz-invariant definition of the cross section in terms of d^3p . The results could thus be interpreted as the massless approximation to d^3p .

The ATLAS detector employs a two-level trigger system: the level-1 hardware stage (L1) and the high-level trigger software stage (HLT). This measurement uses the L1 decision from the minimum-bias trigger scintillators (MBTS), which were replaced between Run 1 and Run 2. The MBTS are mounted at each end of the detector in front of the liquid-argon end-cap calorimeter cryostats at $z = \pm 3.56$ m and segmented into two rings in pseudo-rapidity ($2.07 < |\eta| < 2.76$ and $2.76 < |\eta| < 3.86$). The inner ring is segmented into eight azimuthal sectors while the outer ring is segmented into four azimuthal sectors, giving a total of twelve sectors per side. The MBTS trigger selection used for this paper requires one counter above threshold from either side of the detector and is referred to as a single-arm trigger. The efficiency of this trigger is studied with an independent control trigger. The control trigger selects events randomly at L1 which are then filtered at HLT by requiring at least one reconstructed track with $p_T > 200$ MeV.

3. Monte Carlo event generator simulation

The PYTHIA 8 [12], EPOS [13] and QGSJET-II [14] MC generators are used to correct the data for detector effects and to compare with particle-level corrected data. A brief introduction to the relevant parts of these event generators is given below.

In PYTHIA 8 inclusive hadron–hadron interactions are described by a model that splits the total inelastic cross section into non-diffractive (ND) processes, dominated by t -channel gluon exchange, and diffractive processes involving a colour-singlet exchange. The simulation of ND processes includes multiple parton–parton interactions (MPI). The diffractive processes are further divided into single-diffractive dissociation (SD), where one of the initial protons remains intact and the other is diffractively excited and dissociates, and double-diffractive dissociation (DD) where both protons dissociate. The sample contains approximately 22% SD and 12% DD processes. Such events tend to have large gaps in particle production at central rapidity. A pomeron-based approach is used to describe these events [15].

EPOS provides an implementation of a parton-based Gribov–Regge [16] theory, which is an effective QCD-inspired field theory describing hard and soft scattering simultaneously.

QGSJET-II provides a phenomenological treatment of hadronic and nuclear interactions in the Reggeon field theory framework [17]. The soft and semi-hard parton processes are included in the model within the “semi-hard pomeron” approach. EPOS and QGSJET-II calculations do not rely on the standard parton distribution functions (PDFs) as used in generators such as PYTHIA 8.

Different settings of model parameters optimised to reproduce existing experimental data are used in the simulation. These settings are referred to as tunes. For PYTHIA 8 two tunes are used, A2 [18] and MONASH [19]; for EPOS the LHC [20] tune is used. QGSJET-II uses the default tune from the generator. Each tune utilises 7 TeV minimum-bias data and is summarised in Table 1, together with the version of each generator used to produce the samples. The PYTHIA 8 A2 sample, combined with a single-particle MC simulation used to populate the high- p_T region, is used to derive the detector corrections for these measurements. All the

Table 1

Summary of MC tunes used to compare to the corrected data. The generator and its version are given in the first two columns, the tune name and the PDF used are given in the next two columns.

Generator	Version	Tune	PDF
PYTHIA 8	8.185	A2	MSTW2008Lo [21]
PYTHIA 8	8.186	MONASH	NNPDF2.3Lo [22]
EPOS	LHCv3400	LHC	N/A
QGSJET-II	II-04	default	N/A

events are processed through the ATLAS detector simulation program [23], which is based on GEANT4 [24]. They are then reconstructed and analysed by the same program chain used for the data.

4. Data selection

The data were recorded during a period with a special configuration of the LHC with low beam currents and reduced beam focusing, and thus giving a low expected mean number of interactions per bunch crossing, $\langle\mu\rangle = 0.005$. Events were selected from colliding proton bunches using a trigger which required one or more MBTS counters above threshold on either side of the detector.

Each event is required to contain a primary vertex, reconstructed from at least two tracks with a minimum p_T of 100 MeV, as described in Ref. [25]. To reduce contamination from events with more than one interaction in a bunch crossing, events with a second vertex containing four or more tracks are removed. Events where the second vertex has fewer than four tracks are not removed. These are dominated by contributions where a secondary interaction is reconstructed as another primary vertex or where the primary vertex is split into two vertices, one with few tracks. The fraction of events rejected by the veto on additional vertices due to split vertices or secondary interactions is estimated in the simulation to be 0.02%, which is negligible and therefore ignored.

Track candidates are reconstructed [26,27] in the silicon detectors and then extrapolated to include measurements in the TRT. Events are required to contain at least one selected track, passing the following criteria: $p_T > 500$ MeV and $|\eta| < 2.5$; at least one pixel hit and at least six SCT hits, with the additional requirement of an innermost-pixel-layer hit if expected⁴ (if a hit in the innermost layer is not expected, the next-to-innermost hit is required if expected); $|d_0^{\text{BL}}| < 1.5$ mm, where the transverse impact parameter, d_0^{BL} , is calculated with respect to the measured beam line position; and $|z_0^{\text{BL}} \cdot \sin\theta| < 1.5$ mm, where z_0^{BL} is the difference between the longitudinal position of the track along the beam line at the point where d_0^{BL} is measured and the longitudinal position of the primary vertex, and θ is the polar angle of the track. Finally, in order to remove tracks with mismeasured p_T due to interactions with the material or other effects, the track-fit χ^2 probability is required to be greater than 0.01 for tracks with $p_T > 10$ GeV. There are 8.87 million events selected, containing a total of 106 million selected tracks.

The performance of the ID track reconstruction in the 13 TeV data and its simulation is studied in Ref. [28]. Overall, good agreement between data and simulation is observed. Fig. 1 shows selected performance plots particularly relevant to this analysis. Fig. 1(a) shows the average number of silicon hits as a function of η . There is reasonably good agreement, although discrepancies of up to 2% (in the end-caps) are seen; however, these have a small effect on the track reconstruction efficiency. The discrepancies are due to differences between data and simulation in the number of operational detector elements and an imperfect description of the amount of detector material between the pixel detector and the SCT. The impact on the results of these discrepancies is discussed in Section 6.3. Fig. 1(b) shows the fraction of tracks with a given number of IBL hits per track. There is a difference of 0.5% between data and simulation in the fraction of tracks with zero IBL hits, coming predominantly from a difference in the rate of tracks from secondary particles, which is discussed in more detail in Section 5.

A systematic uncertainty due to the small remaining difference in the efficiency of the requirement of at least one IBL hit is discussed in Section 6. Figs. 1(c) and 1(d) show the d_0^{BL} and $z_0^{\text{BL}} \cdot \sin\theta$ distributions respectively. In these figures the fraction of tracks from secondary particles in simulation is scaled to match the fraction seen in data, and the separate contributions from tracks from primary and secondary particles are shown. This, along with the differences between simulation and data, which have a negligible impact on the analysis, are discussed in Section 5.

5. Background contributions and non-primary tracks

The contribution from non-collision background events, such as proton interactions with residual gas molecules in the beam pipe, is estimated using events that pass the full event selection but occur when only one of the two beams is present. After normalising to the contribution expected in the selected data sample (using the difference in the time of the MBTS hits on each side of the detector, which is possible as background events with hits on only one side are negligible) a contribution of less than 0.01% of events is found from this source, which is negligible and therefore neglected. Background events from cosmic rays, estimated by considering the expected rate of cosmic-ray events compared to the event readout rate, are also found to be negligible and therefore neglected.

The majority of events with more than one interaction in the same bunch crossing are removed by the rejection of events with more than one primary vertex. Some events may survive because the interactions are very close in z and are merged together. The probability to merge vertices is estimated by inspecting the distribution of the difference in the z position of pairs of vertices (Δz). This distribution displays a deficit around $\Delta z = 0$ due to vertex merging. The magnitude of this effect is used to estimate the probability of merging vertices, which is 3.2%. When this is combined with the number of expected additional interactions for $\langle\mu\rangle = 0.005$, the remaining contribution from tracks from additional interactions is found to be less than 0.01%, which is negligible and therefore neglected. The additional tracks in events in which the second vertex has fewer than four associated tracks are mostly rejected by the $z_0^{\text{BL}} \cdot \sin\theta$ requirement, and the remaining contribution is also negligible and neglected.

The contribution from tracks originating from secondary particles is subtracted from the number of reconstructed tracks before correcting for other detector effects. These particles are due to hadronic interactions, photon conversions and decays of long-lived particles. There is also a contribution of less than 0.1% from fake tracks (those formed by a random combination of hits or from a combination of hits from several particles); these are neglected. The contribution of tracks from secondary particles is estimated using simulation predictions for the shapes of the d_0^{BL} distributions for tracks from primary and secondary particles satisfying all track selection criteria except the one on d_0^{BL} . These predictions form templates that are fit to the data in order to extract the relative contribution of tracks from secondary particles. The Gaussian core of the distribution is dominated by the tracks from primary particles, with a width determined by their d_0^{BL} resolution; tracks from secondary particles dominate the tails. The fit is performed in the region $4 < |d_0^{\text{BL}}| < 9.5$ mm, in order to reduce the dependence on the description of the d_0^{BL} resolution, which affects the core of the distribution. From the fit, it was determined that the fraction of tracks from secondary particles in simulation needs to be scaled by a factor 1.38 ± 0.14 . This indicates that $(2.3 \pm 0.6)\%$ of tracks satisfying the final track selection criteria ($|d_0^{\text{BL}}| < 1.5$ mm) originate from secondary particles, where systematic uncertainties are dominant and are discussed below. Of these tracks 6% come

⁴ A hit is expected if the extrapolated track crosses an active region of a pixel module that has not been disabled.

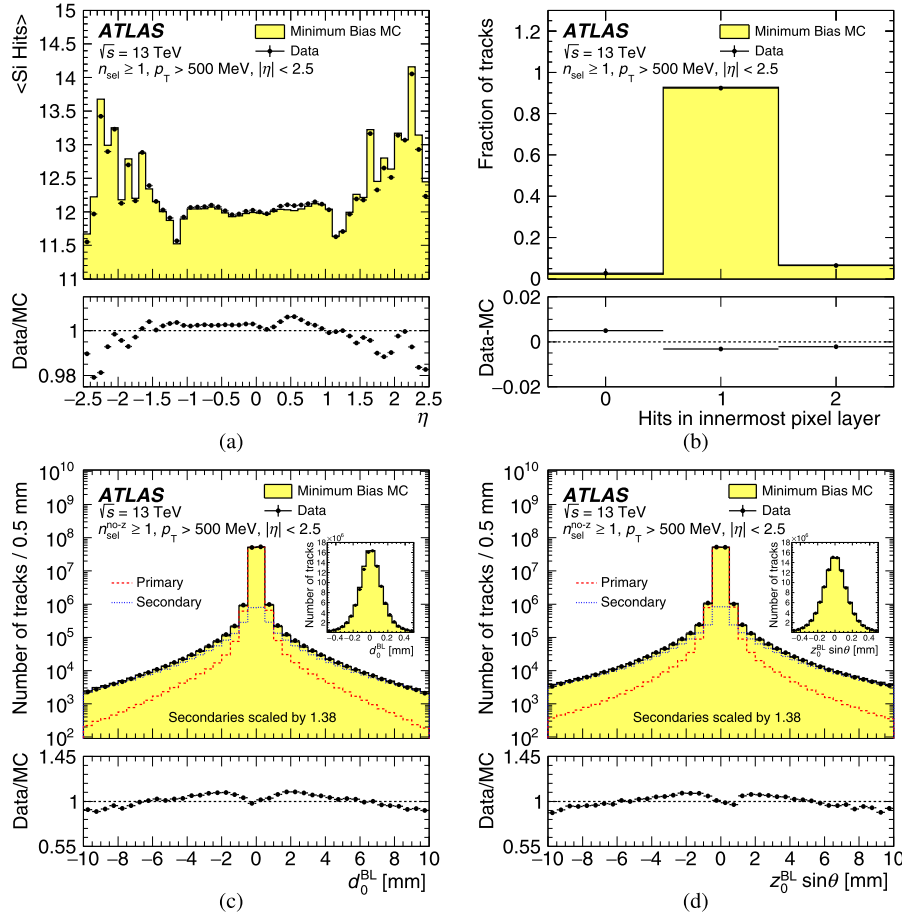


Fig. 1. Comparison between data and PYTHIA 8 A2 simulation for (a) the average number of silicon hits per track, before the requirement on the number of SCT hits is applied, as a function of pseudorapidity, η ; (b) the number of innermost-pixel-layer hits on a track before the requirement on the number of innermost-pixel-layer hits is applied; (c) the transverse impact parameter distribution of the tracks, prior to any requirement on the transverse impact parameter, calculated with respect to the average beam position, d_0^{BL} ; and (d) the difference between the longitudinal position of the track along the beam line at the point where d_0^{BL} is measured and the longitudinal position of the primary vertex projected to the plane transverse to the track direction, $z_0^{\text{BL}} \cdot \sin \theta$, prior to any requirement on $z_0^{\text{BL}} \cdot \sin \theta$. The uncertainties are the statistical uncertainties of the data. In (c) and (d) the separate contributions from tracks coming from primary and secondary particles are also shown and the fraction of secondary particles in the simulation is scaled by 1.38 to match that seen in the data, with the final simulation distributions normalised to the number of tracks in the data. The inserts in the panels for (c) and (d) show the distributions on a linear scale.

from photon conversions and the rest from hadronic interactions or long-lived decays. The description of the η and p_T dependence of this contribution is modelled sufficiently accurately by the simulation that no additional correction is required. Fig. 1(c) shows the d_0^{BL} distribution for data compared to the simulation with the fraction of tracks from secondary particles scaled to the fitted value. A small disagreement is observed in the core of the d_0^{BL} distribution. This has no impact in the tail of the distribution used for the fit. The dominant systematic uncertainty stems from the interpolation of the number of tracks from secondary particles from the fit region to the region $|d_0^{\text{BL}}| < 1.5$ mm. Different generators are used to estimate the interpolation and differences between data and simulation in the shape of the d_0^{BL} distribution in the fit region are considered. Additional, much smaller, systematic uncertainties arise from a variation of the fit range, considering the η dependence of the fitted fractions and from using special simulation samples with varying amounts of detector material.

There is a second source of non-primary particles: charged particles with a mean lifetime $30 < \tau < 300$ ps which, unlike in previous analyses [1], are excluded from the primary-particle definition. These are charged strange baryons that decay after a short flight length and have a very low track reconstruction efficiency. Reconstructed tracks from these particles are treated as background and are subtracted. The fraction of reconstructed tracks coming

from strange baryons is estimated from simulation with EPOS to be $(0.01 \pm 0.01)\%$ on average, with the fraction increasing with track p_T to be $(3 \pm 1)\%$ above 20 GeV. The fraction is much smaller at low p_T due to the extremely low efficiency of reconstructing a track from a particle that decays early in the detector. The systematic uncertainty is taken as the maximum difference between the nominal EPOS prediction and that of PYTHIA 8 A2 or PYTHIA 8 MONASH, which is then symmetrised.

6. Selection efficiency

The data are corrected to obtain inclusive spectra for primary charged particles satisfying the particle-level kinematic requirements. These corrections account for inefficiencies due to trigger selection, vertex and track reconstruction.

In the following sections the methods used to obtain these efficiencies, as well as the systematic uncertainties associated with them, are described.

6.1. Trigger efficiency

The trigger efficiency, $\varepsilon_{\text{trig}}$, is measured from a data sample selected using the control trigger described in Section 2. The requirement of an event primary vertex is removed for these trigger stud-

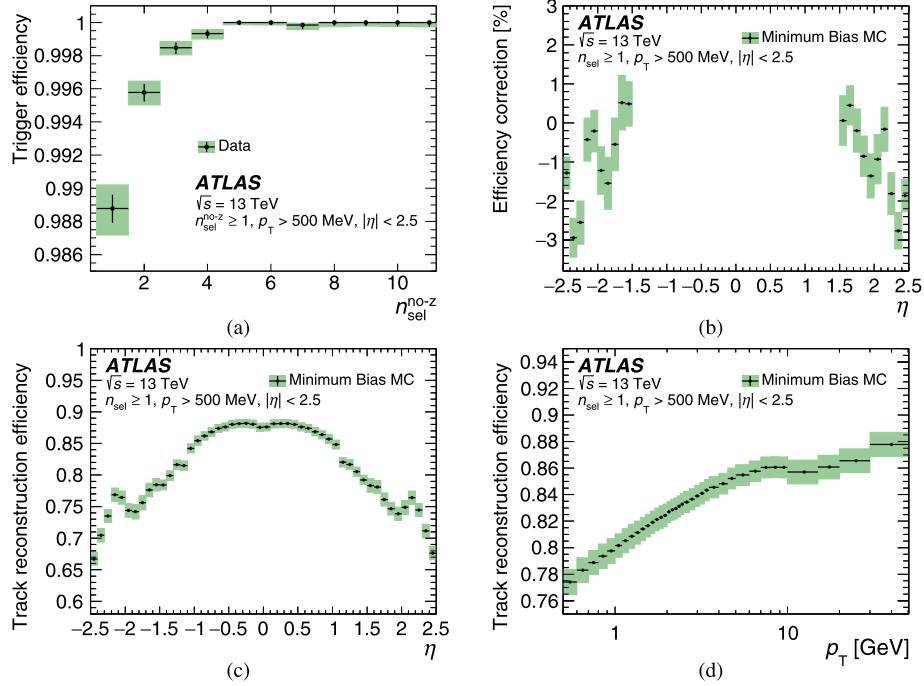


Fig. 2. (a) Trigger efficiency with respect to the event selection, as a function of the number of reconstructed tracks without the $z_0^{\text{BL}} \cdot \sin \theta$ constraint ($n_{\text{sel}}^{\text{no-z}}$). (b) Data-driven correction to the track reconstruction efficiency as a function of pseudorapidity, η . The track reconstruction efficiency after this correction as a function of (c) η and (d) transverse momentum, p_T as predicted by PYTHIA 8 A2 and single-particle simulation. The statistical uncertainties are shown as black vertical bars, the total uncertainties as green shaded areas. (For interpretation of the references to colour in this figure legend, the reader is referred to the web version of this article.)

ies, to account for possible correlations between the trigger and vertex reconstruction efficiencies. The trigger efficiency is therefore parameterised as a function of $n_{\text{sel}}^{\text{no-z}}$, which is defined as the number of tracks passing all of the track selection requirements except for the $z_0^{\text{BL}} \cdot \sin \theta$ constraint, as this requires knowledge of the primary vertex position. The trigger efficiency is taken to be the fraction of events from the control trigger in which the MBTS trigger also accepted the event. This is shown in Fig. 2(a) as a function of $n_{\text{sel}}^{\text{no-z}}$. The efficiency is measured to be just below 99% for $n_{\text{sel}}^{\text{no-z}} = 1$ and it rapidly rises to 100% at higher track multiplicities. The trigger requirement is found to introduce no observable bias in the p_T and η distributions of selected tracks. Systematic uncertainties are estimated from differences in the trigger efficiency measured on each of the two sides of the detector and from a study that assesses the impact of beam-induced background and tracks from secondary particles by varying the impact parameter requirements on selected tracks. The total systematic uncertainty is $\pm 0.15\%$ for $n_{\text{sel}}^{\text{no-z}} = 1$ and it rapidly decreases at higher track multiplicities. This uncertainty is negligible compared to those from other sources and is therefore neglected.

6.2. Vertex reconstruction efficiency

The vertex reconstruction efficiency, ε_{vtx} , is determined from data by taking the ratio of the number of selected events with a reconstructed vertex to the total number of events with the requirement of a primary vertex removed. The expected contribution from beam background events is estimated using the same method as described in Section 5 and subtracted before measuring the efficiency. Like the trigger efficiency, the vertex efficiency is measured in bins of $n_{\text{sel}}^{\text{no-z}}$ as the $z_0^{\text{BL}} \cdot \sin \theta$ constraint cannot be applied to the tracks in this study. The efficiency is measured to be just below 90% for $n_{\text{sel}}^{\text{no-z}} = 1$ and it rapidly rises to 100% at higher track multiplicities. In events with $n_{\text{sel}}^{\text{no-z}} = 1$ the efficiency is also measured as a function of η of the track, and the efficiency increases

monotonically from 81% at $|\eta| = 2.5$ to 93% at $|\eta| = 0$. The systematic uncertainty is estimated from the difference between the vertex reconstruction efficiency measured prior to and after beam background removal. The uncertainty is $\pm 0.1\%$ for $n_{\text{sel}}^{\text{no-z}} = 1$ and rapidly decreases at higher track multiplicities. This uncertainty is negligible compared to those from other sources and is therefore neglected.

6.3. Track reconstruction efficiency

The primary track reconstruction efficiency, ε_{trk} , is determined from the simulation, corrected to account for differences between data and simulation in the amount of detector material between the pixel and SCT detectors in the region $|\eta| > 1.5$. In the other regions of the detector there is an uncertainty due to the knowledge of the detector material that will be discussed below, but no correction is applied. The efficiency is parameterised in two-dimensional bins of p_T and η and is defined as:

$$\varepsilon_{\text{trk}}(p_T, \eta) = \frac{N_{\text{rec}}^{\text{matched}}(p_T, \eta)}{N_{\text{gen}}(p_T, \eta)},$$

where p_T and η are generated particle properties, $N_{\text{rec}}^{\text{matched}}(p_T, \eta)$ is the number of reconstructed tracks matched to a generated primary charged particle and $N_{\text{gen}}(p_T, \eta)$ is the number of generated primary charged particles in that bin. A track is matched to a generated particle if the weighted fraction of hits on the track which originate from that particle exceeds 50%. The hits are weighted such that all subdetectors have the same weight in the sum.

The track reconstruction efficiency depends on the amount of material in the detector, due to particle interactions that lead to efficiency losses. The relatively large amount of material between the pixel and SCT detectors in the region $|\eta| > 1.5$ has changed between Run 1 and Run 2 due to the replacement of some pixel services, which are difficult to simulate accurately. The track reconstruction efficiency in this region is corrected using a method

that compares the efficiency to extend a track reconstructed in the pixel detector into the SCT in data and simulation. Differences in this extension efficiency are sensitive to differences in the amount of material in this region. The correction together with the systematic uncertainty, coming predominantly from the uncertainty of the particle composition in the simulation used to make the measurement, is shown in Fig. 2(b). The uncertainty in the track reconstruction efficiency resulting from this correction is $\pm 0.4\%$ in the region $|\eta| > 1.5$.

The resulting reconstruction efficiency as a function of η integrated over p_T is shown in Fig. 2(c). The track reconstruction efficiency is lower in the region $|\eta| > 1$ due to particles passing through more material in that region. The slight increase in efficiency at $|\eta| \sim 2.2$ is due to the particles passing through an increasing number of layers in the ID end-cap. Fig. 2(d) shows the efficiency as a function of p_T integrated over η .

A good description of the material in the detector in the regions not probed by the method described above (which only probes the material between the pixel and SCT detectors in the region $|\eta| > 1.5$) is needed to obtain a good description of the track reconstruction efficiency. The material within the ID was studied extensively during Run 1 [29], where the amount of material was known to within $\pm 5\%$. This gives rise to a systematic uncertainty in the track reconstruction efficiency of $\pm 0.6\%$ ($\pm 1.2\%$) in the most central (forward) region. Between Run 1 and Run 2 the IBL was installed, the simulation of which must therefore be studied with the Run 2 data. Two data-driven methods are used: a study of secondary vertices from photon conversions ($\gamma \rightarrow e^+e^-$) and a study of secondary vertices from hadronic interactions, where the radial position of the vertex is measured with good precision. Comparisons between data and simulation indicate that the material in the IBL is constrained to within $\pm 10\%$. This leads to an uncertainty in the track reconstruction efficiency of $\pm 0.1\%$ ($\pm 0.2\%$) in the central (forward) region. This uncertainty is added linearly to the uncertainty from constraints from Run 1, to cover the possibility of missing material in the simulation in both cases. The resulting uncertainty is added in quadrature to the uncertainty from the data-driven correction. The total uncertainty due to the imperfect knowledge of the detector material is $\pm 0.7\%$ in the most central region and $\pm 1.5\%$ in the most forward region.

There is a small difference in efficiency, between data and simulation, of the requirement that each reconstructed track has at least one pixel hit, at least six SCT hits, an innermost-pixel-layer hit if expected (if a hit in the innermost layer is not expected, the next-to-innermost hit is required if expected) and a track-fit χ^2 probability greater than 0.01 for tracks with $p_T > 10$ GeV. This difference is assigned as a further systematic uncertainty, amounting to $\pm 0.5\%$ for $p_T < 10$ GeV and $\pm 0.7\%$ for $p_T > 10$ GeV.

The total uncertainty due to the track reconstruction efficiency determination, shown in Figs. 2(c) and 2(d), is obtained by adding all effects in quadrature and is dominated by the uncertainty from the material description.

7. Correction procedure

The following steps are taken to correct the measurements for detector effects.

- All distributions are corrected for the loss of events due to the trigger and vertex requirements by reweighting events according to the function:

$$w_{\text{ev}}(n_{\text{sel}}^{\text{no-z}}, \eta) = \frac{1}{\varepsilon_{\text{trig}}(n_{\text{sel}}^{\text{no-z}})} \cdot \frac{1}{\varepsilon_{\text{vtx}}(n_{\text{sel}}^{\text{no-z}}, \eta)},$$

where the η dependence is only relevant for $n_{\text{sel}}^{\text{no-z}} = 1$, as discussed in Section 6.2.

- The η and p_T distributions of selected tracks are corrected using a track-by-track weight:

$$w_{\text{trk}}(p_T, \eta) = \frac{1 - f_{\text{sec}}(p_T, \eta) - f_{\text{sb}}(p_T) - f_{\text{okr}}(p_T, \eta)}{\varepsilon_{\text{trk}}(p_T, \eta)}$$

where f_{sec} and f_{sb} are the fraction of tracks from secondary particles and from strange baryons respectively, determined as described in Section 5. The fraction of selected tracks for which the corresponding primary particle is outside the kinematic range, $f_{\text{okr}}(p_T, \eta)$, originates from resolution effects and is estimated from the simulation to be 3.5% at $p_T = 500$ MeV, decreasing to 1% for $p_T = 1$ GeV and is only relevant for $2.4 < |\eta| < 2.5$. No additional corrections are needed for the η distribution. For the p_T distribution a Bayesian unfolding [30] is applied to correct the measured track p_T distribution to that for primary particles.

- After applying the trigger and vertex efficiency corrections, the Bayesian unfolding is applied to the multiplicity distribution in order to correct from the observed track multiplicity to the multiplicity of primary charged particles, and therefore the track reconstruction efficiency weight does not need to be applied. The correction procedure also accounts for events that have migrated out of the selected kinematic range ($n_{\text{ch}} \geq 1$).
- The total number of events, N_{ev} , used to normalise the distributions, is defined as the integral of the n_{ch} distribution, after all corrections are applied.
- The dependence of $\langle p_T \rangle$ on n_{ch} is obtained by first separately correcting $\sum_i p_T(i)$ (summing over the p_T of all tracks and all events) versus the number of selected tracks and the total number of tracks in all events versus the number of selected tracks, and then taking the ratio. They are corrected using the appropriate track weights first, followed by the Bayesian unfolding procedure.

Systematic uncertainties in the track reconstruction efficiency, discussed in Section 6, and the fraction of tracks from non-primary particles, discussed in Section 5, give rise to an uncertainty in $w_{\text{trk}}(p_T, \eta)$, directly affecting the η and p_T distributions. For the n_{ch} distribution, where the track weights are not explicitly applied, the effects from uncertainties in these sources are found by modifying the distribution of selected tracks in data. In each multiplicity interval tracks are randomly removed or added with probabilities dependent on the uncertainties in the track weights of tracks populating that bin. This modified distribution is then unfolded and the deviation from the nominal n_{ch} distribution is taken as a systematic uncertainty. An uncertainty from the fact that the correction procedure, when applied to simulated events, does not reproduce exactly the distribution from generated particles (non-closure) is included in all measurements. An additional systematic uncertainty in the measured p_T distribution arises from possible biases and degradation in the p_T measurement. This is quantified by comparing the track hit residuals in data and simulation. The effectiveness of the track-fit χ^2 probability selection in suppressing tracks reconstructed with high momentum but originating from low momentum particles was also considered; it was found that the fraction of these tracks remaining was consistent with predictions from simulation. An uncertainty due to the statistical precision of the check is included for the p_T distribution. Uncertainty sources that also affect N_{ev} partially cancel in the final distributions. A summary of the main systematic uncertainties affecting the η , p_T and n_{ch} distributions is given in Table 2.

Uncertainties in the $\langle p_T \rangle$ vs. n_{ch} measurement are found in the same way as those in the n_{ch} distribution. The dominant uncertainty is from non-closure which varies from $\pm 2\%$ at low n_{ch} to

Table 2Summary of systematic uncertainties on the η , p_T and n_{ch} distributions.

Source	Distribution	Range of values
Track reconstruction efficiency	η	0.5%–1.4%
	p_T	0.7%
	n_{ch}	0%– $^{+17}_{-14}$ %
Non-primaries	η	0.5%
	p_T	0.5%–0.9%
	n_{ch}	0%– $^{+10}_{-8}$ %
Non-closure	η	0.7%
	p_T	0%–2%
	n_{ch}	0%–4%
p_T -bias	p_T	0%–5%
High- p_T	p_T	0%–1%

$\pm 0.5\%$ at high n_{ch} . All other uncertainties largely cancel in the ratio and are negligible. At high n_{ch} the total uncertainty is dominated by the statistical uncertainty.

8. Results

The corrected distributions for primary charged particles in events with $n_{ch} \geq 1$ in the kinematic range $p_T > 500$ MeV and $|\eta| < 2.5$ are shown in Fig. 3. In most regions of all distributions the dominant uncertainty comes from the track reconstruction efficiency. The results are compared to predictions of models tuned to a wide range of measurements. The measured distributions are presented as inclusive distributions with corrections that rely minimally on the MC model used, in order to facilitate an accurate comparison with predictions.

Fig. 3(a) shows the multiplicity of charged particles as a function of pseudorapidity. The mean particle density is roughly constant at 2.9 for $|\eta| < 1.0$ and decreases at higher values of $|\eta|$. EPOS describes the data for $|\eta| < 1.0$, and predicts a slightly larger multiplicity at larger $|\eta|$ values. QGSJET-II and PYTHIA 8 MONASH predict

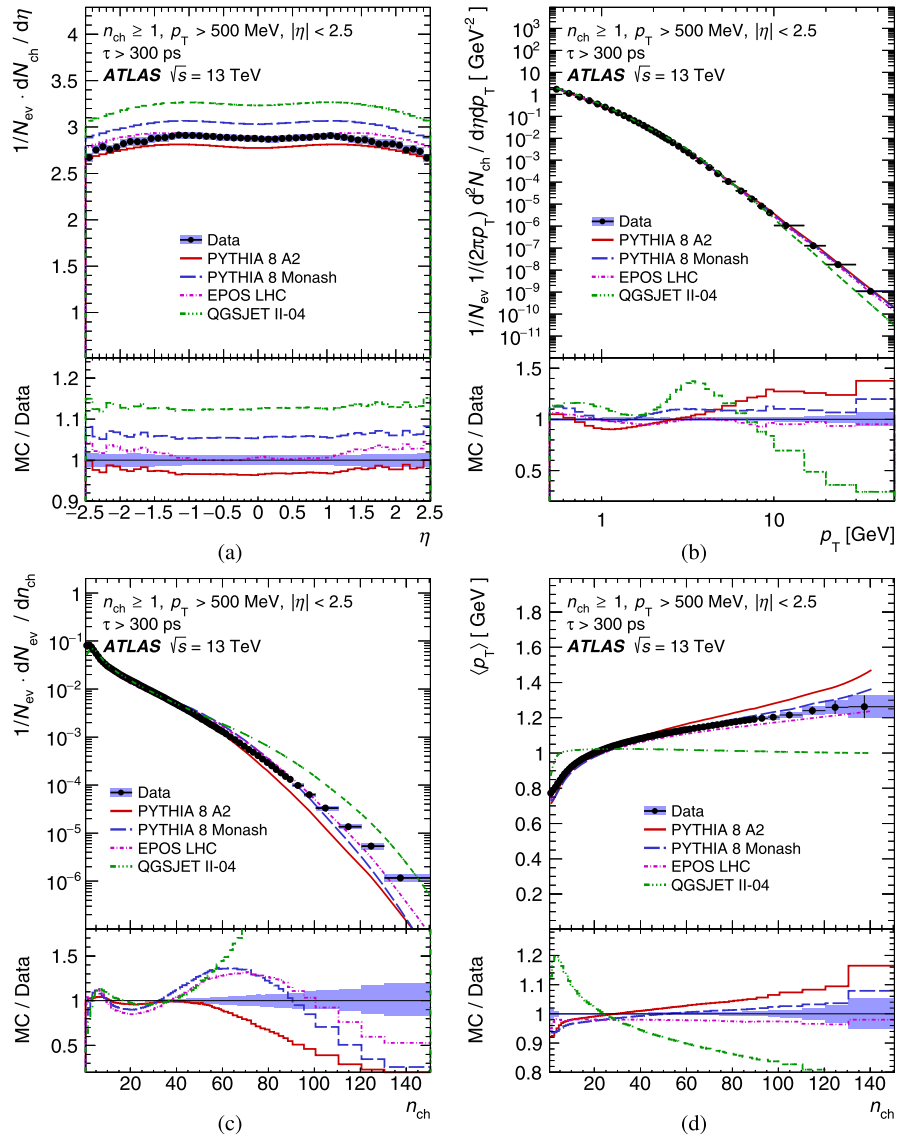


Fig. 3. Primary-charged-particle multiplicities as a function of (a) pseudorapidity, η , and (b) transverse momentum, p_T ; (c) the multiplicity, n_{ch} , distribution and (d) the mean transverse momentum, $\langle p_T \rangle$, versus n_{ch} in events with $n_{ch} \geq 1$, $p_T > 500$ MeV and $|\eta| < 2.5$. The dots represent the data and the curves represent the predictions from different MC models. The x -value in each bin corresponds to the bin centroid. The vertical bars represent the statistical uncertainties, while the shaded areas show statistical and systematic uncertainties added in quadrature. The bottom panel in each figure shows the ratio of the MC simulation to data. Since the bin centroid is different for data and simulation, the values of the ratio correspond to the averages of the bin content.

multiplicities that are too large by approximately 15% and 5% respectively. PYTHIA 8 A₂ predicts a multiplicity that is 3% too low in the central region, but describes the data well in the forward region.

Fig. 3(b) shows the charged-particle transverse momentum distribution. EPOS describes the data well over the entire p_T spectrum. The PYTHIA 8 tunes describe the data reasonably well, but are slightly above the data in the high- p_T region. QGSJET-II gives a poor prediction over the entire spectrum, overshooting the data in the low- p_T region and undershooting it in the high- p_T region.

Fig. 3(c) shows the charged-particle multiplicity distribution. The high- n_{ch} region has significant contributions from events with numerous MPI. PYTHIA 8 A₂ describes the data in the region $n_{ch} < 50$, but predicts too few events at larger n_{ch} values. PYTHIA 8 MONASH, EPOS and QGSJET-II describe the data reasonably well in the region $n_{ch} < 30$ but predict too many events in the mid- n_{ch} region, with PYTHIA 8 MONASH and EPOS predicting too few events in the region $n_{ch} > 100$ while QGSJET-II continues to be above the data.

Fig. 3(d) shows the mean transverse momentum versus the charged-particle multiplicity. The $\langle p_T \rangle$ rises with n_{ch} , from 0.8 to 1.2 GeV. This increase is expected due to colour coherence effects being important in dense parton environments and is modelled by a colour reconnection mechanism in PYTHIA 8 or by the hydrodynamical evolution model used in EPOS. If the high- n_{ch} region is assumed to be dominated by events with numerous MPI, without colour coherence effects the $\langle p_T \rangle$ is approximately independent of n_{ch} . Including colour coherence effects leads to fewer additional charged particles produced with every additional MPI, with an equally large p_T to be shared among the produced hadrons [31]. EPOS predicts a slightly lower $\langle p_T \rangle$, but describes the dependence on n_{ch} very well. The PYTHIA 8 tunes predict a steeper rise of $\langle p_T \rangle$ with n_{ch} than the data, predicting lower values in the low- n_{ch} region and higher values in the high- n_{ch} region. QGSJET-II predicts a $\langle p_T \rangle$ of ~ 1 GeV, with very little dependence on n_{ch} ; this is expected as it contains no model for colour coherence effects.

In summary, EPOS and the PYTHIA 8 tunes describe the data most accurately, with EPOS reproducing the η and p_T distributions and the $\langle p_T \rangle$ vs. n_{ch} the best and PYTHIA 8 A₂ describing the multiplicity the best in the low- and mid- n_{ch} regions. QGSJET-II provides an inferior description of the data.

The mean number of primary charged particles in the central region is computed by averaging over $|\eta| < 0.2$ to be 2.874 ± 0.001 (stat.) ± 0.033 (syst.). This measurement is then corrected for the contribution from strange baryons and compared to previous measurements [1] at different \sqrt{s} values in Fig. 4 together with the MC predictions. The correction factor for strange baryons depends on the MC model used and is found to be 1.0241 ± 0.0003 (EPOS), 1.0150 ± 0.0004 (PYTHIA 8 MONASH) and 1.0151 ± 0.0002 (PYTHIA 8 A₂), where the uncertainties are statistical. QGSJET-II does not include charged strange baryons. The prediction from EPOS is used to perform the extrapolation and the deviation from the PYTHIA 8 MONASH prediction is taken as a systematic uncertainty and symmetrised to give 1.024 ± 0.009 .

The mean number of primary charged particles increases by a factor of 2.2 when \sqrt{s} increases by a factor of about 14 from 0.9 TeV to 13 TeV. EPOS and PYTHIA 8 A₂ describe the dependence on \sqrt{s} very well, while PYTHIA 8 MONASH and QGSJET-II predict a steeper rise in multiplicity with \sqrt{s} .

9. Conclusion

Primary-charged-particle multiplicity measurements with the ATLAS detector using proton–proton collisions delivered by the LHC at $\sqrt{s} = 13$ TeV are presented. From a data sample correspond-

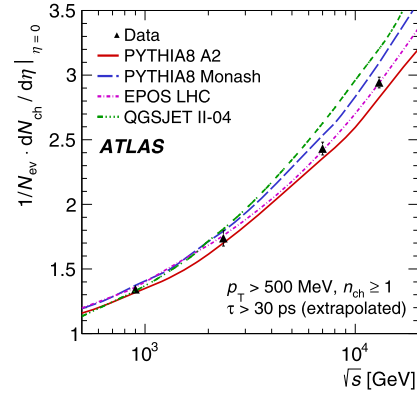


Fig. 4. The average primary-charged-particle multiplicity in pp interactions per unit of pseudorapidity, η , for $|\eta| < 0.2$ as a function of the centre-of-mass energy. The values at centre-of-mass energies other than 13 TeV are taken from Ref. [1]. Charged strange baryons are included in the definition of primary particles. The data are compared to various particle-level MC predictions. The vertical error bars on the data represent the total uncertainty.

ing to an integrated luminosity of $170 \mu\text{b}^{-1}$, nearly nine million inelastic interactions with at least one reconstructed track with $|\eta| < 2.5$ and $p_T > 500$ MeV are analysed. The results highlight clear differences between MC models and the measured distributions. Among the models considered EPOS reproduces the data the best, PYTHIA 8 A₂ and MONASH give reasonable descriptions of the data and QGSJET-II provides the worst description of the data.

Acknowledgements

We thank CERN for the very successful operation of the LHC, as well as the support staff from our institutions without whom ATLAS could not be operated efficiently.

We acknowledge the support of ANPCyT, Argentina; YerPhI, Armenia; ARC, Australia; BMWFW and FWF, Austria; ANAS, Azerbaijan; SSTC, Belarus; CNPq and FAPESP, Brazil; NSERC, NRC and CFI, Canada; CERN; CONICYT, Chile; CAS, MOST and NSFC, China; COLCIENCIAS, Colombia; MSMT CR, MPO CR and VSC CR, Czech Republic; DNRF, DNSRC and Lundbeck Foundation, Denmark; IN2P3-CNRS, CEA-DSM/IRFU, France; GNSF, Georgia; BMBF, HGF, and MPG, Germany; GSRT, Greece; RGC, Hong Kong SAR, China; ISF, I-CORE and Benoziyo Center, Israel; INFN, Italy; MEXT and JSPS, Japan; CNRST, Morocco; FOM and NWO, Netherlands; RCN, Norway; MNiSW and NCN, Poland; FCT, Portugal; MNE/IFA, Romania; MES of Russia and NRC KI, Russian Federation; JINR; MESTD, Serbia; MSSR, Slovakia; ARRS and MIZŠ, Slovenia; DST/NRF, South Africa; MINECO, Spain; SRC and Wallenberg Foundation, Sweden; SERI, SNSF and Cantons of Bern and Geneva, Switzerland; MOST, Taiwan; TAEK, Turkey; STFC, United Kingdom; DOE and NSF, United States of America. In addition, individual groups and members have received support from BCKDF, the Canada Council, Canarie, CRC, Compute Canada, FQRNT, and the Ontario Innovation Trust, Canada; EPLANET, ERC, FP7, Horizon 2020 and Marie Skłodowska-Curie Actions, European Union; Investissements d'Avenir Labex and Idex, ANR, Region Auvergne and Fondation Partager le Savoir, France; DFG and AvH Foundation, Germany; Herakleitos, Thales and Aristeia programmes co-financed by EU-ESF and the Greek NSRF; BSF, GIF and Minerva, Israel; BRF, Norway; the Royal Society and Leverhulme Trust, United Kingdom.

The crucial computing support from all WLCG partners is acknowledged gratefully, in particular from CERN and the ATLAS Tier-1 facilities at TRIUMF (Canada), NDGF (Denmark, Norway, Sweden), CC-IN2P3 (France), KIT/GridKA (Germany), INFN-CNAF (Italy),

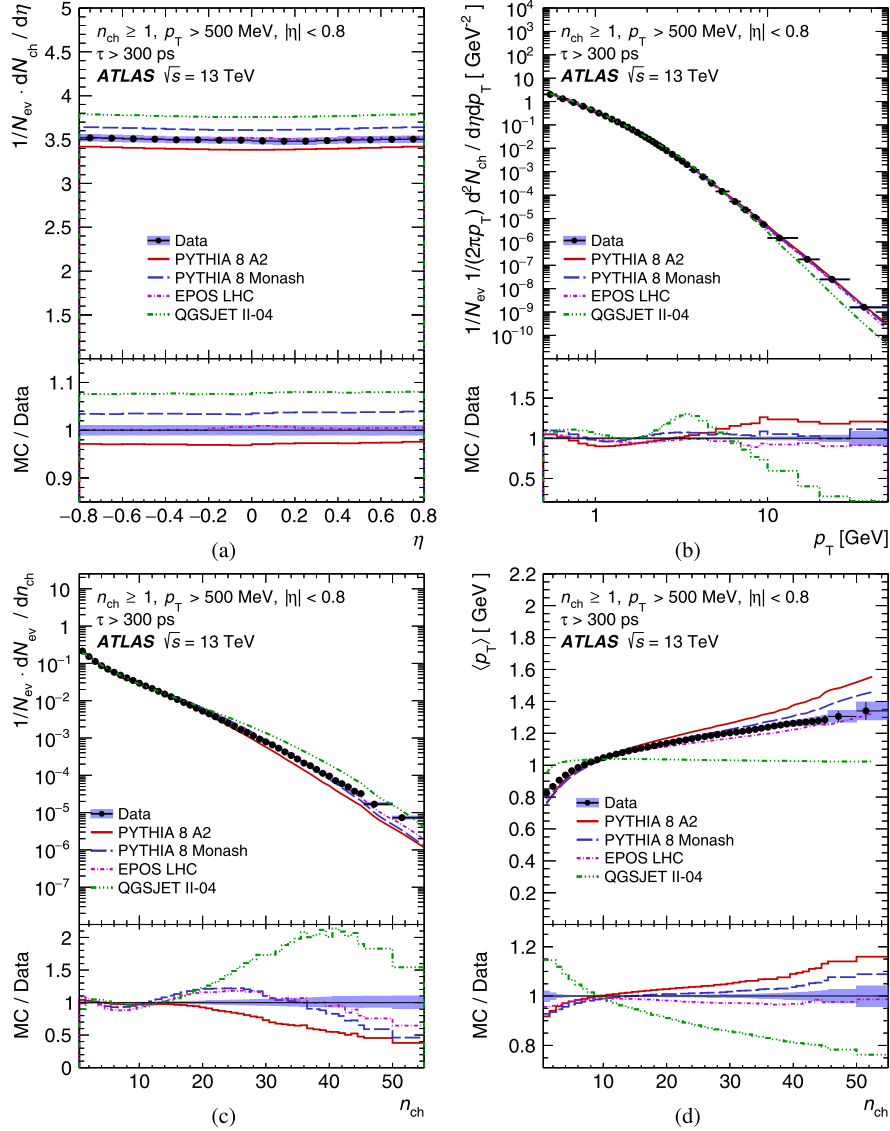


Fig. 5. Primary-charged-particle multiplicities as a function of (a) pseudorapidity, η , and (b) transverse momentum, p_T ; (c) the multiplicity, n_{ch} , distribution and (d) the mean transverse momentum, $\langle p_T \rangle$, versus n_{ch} in events with $n_{ch} \geq 1$, $p_T > 500$ MeV and $|\eta| < 0.8$. The dots represent the data and the curves the predictions from different MC models. The x -value in each bin corresponds to the bin centroid. The vertical bars represent the statistical uncertainties, while the shaded areas show statistical and systematic uncertainties added in quadrature. The bottom panel in each figure shows the ratio of the MC simulation over the data. Since the bin centroid is different for data and simulation, the values of the ratio correspond to the averages of the bin content.

NL-T1 (Netherlands), PIC (Spain), ASGC (Taiwan), RAL (UK) and BNL (USA) and in the Tier-2 facilities worldwide.

Appendix A. Results in a common phase space

The corrected distributions for primary charged particles in events with $n_{ch} \geq 1$ in the kinematic range $p_T > 500$ MeV and $|\eta| < 0.8$ are shown in Fig. 5. This is the phase space that is common to the ATLAS, CMS and ALICE experiments.

The method used to correct the distributions and obtain the systematic uncertainties is exactly the same as that used for the results with $|\eta| < 2.5$, but obtained using the $|\eta| < 0.8$ selection.

Fig. 5(a) shows the primary-charged-particle multiplicity as a function of pseudorapidity, where the mean particle density is roughly 3.5, larger than in the main phase space due to the tighter restriction of at least one primary charged particle with $|\eta| < 0.8$. The p_T and n_{ch} distributions are shown in Figs. 5(b) and 5(c) re-

spectively and the $\langle p_T \rangle$ as a function of n_{ch} is shown in Fig. 5(d). The level of agreement between the data and MC generator predictions follows the same pattern as seen in the main phase space.

References

- [1] ATLAS Collaboration, Charged-particle multiplicities in pp interactions measured with the ATLAS detector at the LHC, *New J. Phys.* 13 (2011) 053033, arXiv:1012.5104 [hep-ex].
- [2] CMS Collaboration, Charged particle multiplicities in pp interactions at $\sqrt{s} = 0.9$, 2.36, and 7 TeV, *J. High Energy Phys.* 1101 (2011) 079, arXiv:1011.5531 [hep-ex].
- [3] CMS Collaboration, Transverse momentum and pseudorapidity distributions of charged hadrons in pp collisions at $\sqrt{s} = 7$ TeV, *Phys. Rev. Lett.* 105 (2010) 022002, arXiv:1005.3299 [hep-ex].
- [4] CMS Collaboration, Transverse momentum and pseudorapidity distributions of charged hadrons in pp collisions at $\sqrt{s} = 0.9$ and 2.36 TeV, *J. High Energy Phys.* 1002 (2010) 041, arXiv:1002.0621 [hep-ex].

- [5] ALICE Collaboration, K. Aamodt, et al., Charged-particle multiplicity measured in proton–proton collisions at $\sqrt{s} = 7$ TeV with ALICE at LHC, *Eur. Phys. J. C* 68 (2010) 345–354, arXiv:1004.3514 [hep-ex].
- [6] CDF Collaboration, T. Aaltonen, et al., Measurement of particle production and inclusive differential cross sections in $p\bar{p}$ collisions at $\sqrt{s} = 1.96$ TeV, *Phys. Rev. D* 79 (2009) 112005, arXiv:0904.1098 [hep-ex].
- [7] CMS Collaboration, Pseudorapidity distribution of charged hadrons in proton–proton collisions at $\sqrt{s} = 13$ TeV, *Phys. Lett. B* 751 (2015) 143, arXiv:1507.05915 [hep-ex].
- [8] ATLAS Collaboration, The ATLAS experiment at the CERN Large Hadron Collider, *J. Instrum.* 3 (2008) S08003.
- [9] CMS Collaboration, The CMS experiment at the CERN LHC, *J. Instrum.* 3 (2008) S08004.
- [10] ALICE Collaboration, K. Aamodt, et al., The ALICE experiment at the CERN LHC, *J. Instrum.* 3 (2008) S08002.
- [11] ATLAS Collaboration, ATLAS insertable B-layer technical design report, CERN-LHCC-2010-013, ATLAS-TDR-19, <http://cdsweb.cern.ch/record/1291633>, 2010, CERN-LHCC-2012-009, ATLAS-TDR-19-ADD-1; ATLAS Collaboration, ATLAS insertable B-layer technical design report addendum, CERN-LHCC-2012-009, ATLAS-TDR-19-ADD-1, addendum to CERN-LHCC-2010-013, ATLAS-TDR-019, <http://cdsweb.cern.ch/record/1451888>, 2012.
- [12] T. Sjöstrand, S. Mrenna, P.Z. Skands, A brief introduction to PYTHIA 8.1, *Comput. Phys. Commun.* 178 (2008) 852, arXiv:0710.3820 [hep-ph].
- [13] S. Porteboeuf, T. Pierog, K. Werner, Producing hard processes regarding the complete event: the EPOS event generator, arXiv:1006.2967 [hep-ph], 2010.
- [14] S. Ostapchenko, Monte Carlo treatment of hadronic interactions in enhanced Pomeron scheme: QGSJET-II model, *Phys. Rev. D* 83 (2011) 014018, arXiv:1010.1869 [hep-ph].
- [15] R. Corke, T. Sjöstrand, Interleaved parton showers and tuning prospects, *J. High Energy Phys.* 1103 (2011) 032, arXiv:1011.1759.
- [16] H.J. Drescher, M. Hladik, S. Ostapchenko, T. Pierog, K. Werner, Parton-based Gribov–Regge theory, *Phys. Rep.* 350 (2001) 93, arXiv:hep-ph/0007198.
- [17] V.N. Gribov, A reggeon diagram technique, *JETP* 26 (1968) 414.
- [18] ATLAS Collaboration, Further ATLAS tunes of Pythia 6 and Pythia 8, ATL-PHYS-PUB-2011-014, <http://cds.cern.ch/record/1400677>, 2011.
- [19] P. Skands, S. Carrazza, J. Rojo, Tuning PYTHIA 8.1: the Monash 2013 Tune, *Eur. Phys. J. C* 74 (2014) 3024, arXiv:1404.5630 [hep-ph].
- [20] T. Pierog, I. Karpenko, J. Katzy, E. Yatsenko, K. Werner, EPOS LHC: test of collective hadronization with LHC data, arXiv:1306.0121 [hep-ph], 2013.
- [21] A.D. Martin, W.J. Stirling, R.S. Thorne, G. Watt, Parton distributions for the LHC, *Eur. Phys. J. C* 63 (2009) 189, arXiv:0901.0002 [hep-ph].
- [22] NNPDF Collaboration, R.D. Ball, et al., Parton distributions with LHC data, *Nucl. Phys. B* 867 (2013) 244, arXiv:1207.1303 [hep-ph].
- [23] ATLAS Collaboration, The ATLAS simulation infrastructure, *Eur. Phys. J. C* 70 (2010) 823, arXiv:1005.4568 [physics.ins-det].
- [24] GEANT4 Collaboration, S. Agostinelli, et al., GEANT4 – A simulation toolkit, *Nucl. Instrum. Methods Phys. Res., Sect. A, Accel. Spectrom. Detect. Assoc. Equip.* 506 (2003) 250.
- [25] G. Piacquadio, K. Prokofiev, A. Wildauer, Primary vertex reconstruction in the ATLAS experiment at LHC, *J. Phys. Conf. Ser.* 119 (2008) 032033.
- [26] T. Cornelissen, et al., Concepts, design and implementation of the ATLAS New Tracking (NEWT), ATL-SOFT-PUB-2007-007, <http://cdsweb.cern.ch/record/1020106>, 2007.
- [27] T. Cornelissen, et al., The new ATLAS track reconstruction (NEWT), *J. Phys. Conf. Ser.* 119 (2008) 032014.
- [28] ATLAS Collaboration, Track reconstruction performance of the ATLAS inner detector at $\sqrt{s} = 13$ TeV, ATL-PHYS-PUB-2015-018, <http://cds.cern.ch/record/2037683>, 2015.
- [29] ATLAS Collaboration, A study of the material in the ATLAS inner detector using secondary hadronic interactions, *J. Instrum.* 7 (2012) P01013, arXiv:1110.6191 [hep-ex].
- [30] G. D’Agostini, A multidimensional unfolding method based on Bayes’ theorem, *Nucl. Instrum. Methods Phys. Res., Sect. A, Accel. Spectrom. Detect. Assoc. Equip.* 362 (1995) 487–498.
- [31] T. Sjöstrand, Colour reconnection and its effects on precise measurements at the LHC, arXiv:1310.8073 [hep-ph], 2013.

ATLAS Collaboration

G. Aad⁸⁶, B. Abbott¹¹³, J. Abdallah¹⁵¹, O. Abdinov¹¹, B. Abeloos¹¹⁷, R. Aben¹⁰⁷, M. Abolins⁹¹, O.S. AbouZeid¹³⁷, N.L. Abraham¹⁴⁹, H. Abramowicz¹⁵³, H. Abreu¹⁵², R. Abreu¹¹⁶, Y. Abulaiti^{146a,146b}, B.S. Acharya^{163a,163b,a}, L. Adamczyk^{39a}, D.L. Adams²⁶, J. Adelman¹⁰⁸, S. Adomeit¹⁰⁰, T. Adye¹³¹, A.A. Affolder⁷⁵, T. Agatonovic-Jovin¹³, J. Agricola⁵⁵, J.A. Aguilar-Saavedra^{126a,126f}, S.P. Ahlen²³, F. Ahmadov^{66,b}, G. Aielli^{133a,133b}, H. Akerstedt^{146a,146b}, T.P.A. Åkesson⁸², A.V. Akimov⁹⁶, G.L. Alberghi^{21a,21b}, J. Albert¹⁶⁸, S. Albrand⁵⁶, M.J. Alconada Verzini⁷², M. Aleksa³¹, I.N. Aleksandrov⁶⁶, C. Alexa^{27b}, G. Alexander¹⁵³, T. Alexopoulos¹⁰, M. Alhroob¹¹³, M. Aliev^{74a,74b}, G. Alimonti^{92a}, J. Alison³², S.P. Alkire³⁶, B.M.M. Allbrooke¹⁴⁹, B.W. Allen¹¹⁶, P.P. Allport¹⁸, A. Aloisio^{104a,104b}, A. Alonso³⁷, F. Alonso⁷², C. Alpigiani¹³⁸, B. Alvarez Gonzalez³¹, D. Álvarez Piqueras¹⁶⁶, M.G. Alviggi^{104a,104b}, B.T. Amadio¹⁵, K. Amako⁶⁷, Y. Amaral Coutinho^{25a}, C. Amelung²⁴, D. Amidei⁹⁰, S.P. Amor Dos Santos^{126a,126c}, A. Amorim^{126a,126b}, S. Amoroso³¹, N. Amram¹⁵³, G. Amundsen²⁴, C. Anastopoulos¹³⁹, L.S. Ancu⁵⁰, N. Andari¹⁰⁸, T. Andeen³², C.F. Anders^{59b}, G. Anders³¹, J.K. Anders⁷⁵, K.J. Anderson³², A. Andreazza^{92a,92b}, V. Andrei^{59a}, S. Angelidakis⁹, I. Angelozzi¹⁰⁷, P. Anger⁴⁵, A. Angerami³⁶, F. Anghinolfi³¹, A.V. Anisenkov^{109,c}, N. Anjos¹², A. Annovi^{124a,124b}, M. Antonelli⁴⁸, A. Antonov⁹⁸, J. Antos^{144b}, F. Anulli^{132a}, M. Aoki⁶⁷, L. Aperio Bella¹⁸, G. Arabidze⁹¹, Y. Arai⁶⁷, J.P. Araque^{126a}, A.T.H. Arce⁴⁶, F.A. Arduh⁷², J-F. Arguin⁹⁵, S. Argyropoulos⁶⁴, M. Arik^{19a}, A.J. Armbruster³¹, L.J. Armitage⁷⁷, O. Arnaez³¹, H. Arnold⁴⁹, M. Arratia²⁹, O. Arslan²², A. Artamonov⁹⁷, G. Artoni¹²⁰, S. Artz⁸⁴, S. Asai¹⁵⁵, N. Asbah⁴³, A. Ashkenazi¹⁵³, B. Åsman^{146a,146b}, L. Asquith¹⁴⁹, K. Assamagan²⁶, R. Astalos^{144a}, M. Atkinson¹⁶⁵, N.B. Atlay¹⁴¹, K. Augsten¹²⁸, G. Avolio³¹, B. Axen¹⁵, M.K. Ayoub¹¹⁷, G. Azuelos^{95,d}, M.A. Baak³¹, A.E. Baas^{59a}, M.J. Baca¹⁸, H. Bachacou¹³⁶, K. Bachas^{74a,74b}, M. Backes³¹, M. Backhaus³¹, P. Bagiacchi^{132a,132b}, P. Bagnaia^{132a,132b}, Y. Bai^{34a}, J.T. Baines¹³¹, O.K. Baker¹⁷⁵, E.M. Baldin^{109,c}, P. Balek¹²⁹, T. Balestri¹⁴⁸, F. Balli¹³⁶, W.K. Balunas¹²², E. Banas⁴⁰, Sw. Banerjee^{172,e}, A.A.E. Bannoura¹⁷⁴, L. Barak³¹, E.L. Barberio⁸⁹, D. Barberis^{51a,51b}, M. Barbero⁸⁶, T. Barillari¹⁰¹, M. Barisonzi^{163a,163b}, T. Barklow¹⁴³, N. Barlow²⁹, S.L. Barnes⁸⁵, B.M. Barnett¹³¹, R.M. Barnett¹⁵, Z. Barnovska⁵, A. Baroncelli^{134a}, G. Barone²⁴, A.J. Barr¹²⁰, L. Barranco Navarro¹⁶⁶, F. Barreiro⁸³, J. Barreiro Guimarães da Costa^{34a}, R. Bartoldus¹⁴³, A.E. Barton⁷³, P. Bartos^{144a}, A. Basalaev¹²³, A. Bassalat¹¹⁷, A. Basye¹⁶⁵, R.L. Bates⁵⁴, S.J. Batista¹⁵⁸, J.R. Batley²⁹, M. Battaglia¹³⁷, M. Bauce^{132a,132b}, F. Bauer¹³⁶, H.S. Bawa^{143,f}, J.B. Beacham¹¹¹, M.D. Beattie⁷³, T. Beau⁸¹,

P.H. Beauchemin¹⁶¹, P. Bechtle²², H.P. Beck^{17,g}, K. Becker¹²⁰, M. Becker⁸⁴, M. Beckingham¹⁶⁹, C. Becot¹¹⁰, A.J. Beddall^{19e}, A. Beddall^{19b}, V.A. Bednyakov⁶⁶, M. Bedognetti¹⁰⁷, C.P. Bee¹⁴⁸, L.J. Beemster¹⁰⁷, T.A. Beermann³¹, M. Begel²⁶, J.K. Behr⁴³, C. Belanger-Champagne⁸⁸, A.S. Bell⁷⁹, W.H. Bell⁵⁰, G. Bella¹⁵³, L. Bellagamba^{21a}, A. Bellerive³⁰, M. Bellomo⁸⁷, K. Belotskiy⁹⁸, O. Beltramello³¹, N.L. Belyaev⁹⁸, O. Benary¹⁵³, D. Bencheekroun^{135a}, M. Bender¹⁰⁰, K. Bendtz^{146a,146b}, N. Benekos¹⁰, Y. Benhammou¹⁵³, E. Benhar Noccioli¹⁷⁵, J. Benitez⁶⁴, J.A. Benitez Garcia^{159b}, D.P. Benjamin⁴⁶, J.R. Bensinger²⁴, S. Bentvelsen¹⁰⁷, L. Beresford¹²⁰, M. Beretta⁴⁸, D. Berge¹⁰⁷, E. Bergeaas Kuutmann¹⁶⁴, N. Berger⁵, F. Berghaus¹⁶⁸, J. Beringer¹⁵, S. Berlendis⁵⁶, N.R. Bernard⁸⁷, C. Bernius¹¹⁰, F.U. Bernlochner²², T. Berry⁷⁸, P. Berta¹²⁹, C. Bertella⁸⁴, G. Bertoli^{146a,146b}, F. Bertolucci^{124a,124b}, I.A. Bertram⁷³, C. Bertsche¹¹³, D. Bertsche¹¹³, G.J. Besjes³⁷, O. Bessidskaia Bylund^{146a,146b}, M. Bessner⁴³, N. Besson¹³⁶, C. Betancourt⁴⁹, S. Bethke¹⁰¹, A.J. Bevan⁷⁷, W. Bhimji¹⁵, R.M. Bianchi¹²⁵, L. Bianchini²⁴, M. Bianco³¹, O. Biebel¹⁰⁰, D. Biedermann¹⁶, R. Bielski⁸⁵, N.V. Biesuz^{124a,124b}, M. Biglietti^{134a}, J. Bilbao De Mendizabal⁵⁰, H. Bilokon⁴⁸, M. Bindi⁵⁵, S. Binet¹¹⁷, A. Bingul^{19b}, C. Bini^{132a,132b}, S. Biondi^{21a,21b}, D.M. Bjergaard⁴⁶, C.W. Black¹⁵⁰, J.E. Black¹⁴³, K.M. Black²³, D. Blackburn¹³⁸, R.E. Blair⁶, J.-B. Blanchard¹³⁶, J.E. Blanco⁷⁸, T. Blazek^{144a}, I. Bloch⁴³, C. Blocker²⁴, W. Blum^{84,*}, U. Blumenschein⁵⁵, S. Blunier^{33a}, G.J. Bobbink¹⁰⁷, V.S. Bobrovnikov^{109,c}, S.S. Bocchetta⁸², A. Bocci⁴⁶, C. Bock¹⁰⁰, M. Boehler⁴⁹, D. Boerner¹⁷⁴, J.A. Bogaerts³¹, D. Bogavac¹³, A.G. Bogdanchikov¹⁰⁹, C. Bohm^{146a}, V. Boisvert⁷⁸, T. Bold^{39a}, V. Boldea^{27b}, A.S. Boldyrev^{163a,163c}, M. Bomben⁸¹, M. Bona⁷⁷, M. Boonekamp¹³⁶, A. Borisov¹³⁰, G. Borissov⁷³, J. Bortfeldt¹⁰⁰, D. Bortoletto¹²⁰, V. Bortolotto^{61a,61b,61c}, K. Bos¹⁰⁷, D. Boscherini^{21a}, M. Bosman¹², J.D. Bossio Sola²⁸, J. Boudreau¹²⁵, J. Bouffard², E.V. Bouhova-Thacker⁷³, D. Boumediene³⁵, C. Bourdarios¹¹⁷, S.K. Boutle⁵⁴, A. Boveia³¹, J. Boyd³¹, I.R. Boyko⁶⁶, J. Bracinik¹⁸, A. Brandt⁸, G. Brandt⁵⁵, O. Brandt^{59a}, U. Bratzler¹⁵⁶, B. Brau⁸⁷, J.E. Brau¹¹⁶, H.M. Braun^{174,*}, W.D. Breaden Madden⁵⁴, K. Brendlinger¹²², A.J. Brennan⁸⁹, L. Brenner¹⁰⁷, R. Brenner¹⁶⁴, S. Bressler¹⁷¹, T.M. Bristow⁴⁷, D. Britton⁵⁴, D. Britzger⁴³, F.M. Brochu²⁹, I. Brock²², R. Brock⁹¹, G. Brooijmans³⁶, T. Brooks⁷⁸, W.K. Brooks^{33b}, J. Brosamer¹⁵, E. Brost¹¹⁶, J.H. Broughton¹⁸, P.A. Bruckman de Renstrom⁴⁰, D. Bruncko^{144b}, R. Bruneliere⁴⁹, A. Bruni^{21a}, G. Bruni^{21a}, B.H. Brunt²⁹, M. Bruschi^{21a}, N. Bruscino²², P. Bryant³², L. Bryngemark⁸², T. Buanes¹⁴, Q. Buat¹⁴², P. Buchholz¹⁴¹, A.G. Buckley⁵⁴, I.A. Budagov⁶⁶, F. Buehrer⁴⁹, M.K. Bugge¹¹⁹, O. Bulekov⁹⁸, D. Bullock⁸, H. Burckhart³¹, S. Burdin⁷⁵, C.D. Burgard⁴⁹, B. Burghgrave¹⁰⁸, K. Burka⁴⁰, S. Burke¹³¹, I. Burmeister⁴⁴, E. Busato³⁵, D. Büscher⁴⁹, V. Büscher⁸⁴, P. Bussey⁵⁴, J.M. Butler²³, A.I. Butt³, C.M. Buttar⁵⁴, J.M. Butterworth⁷⁹, P. Butti¹⁰⁷, W. Buttinger²⁶, A. Buzatu⁵⁴, A.R. Buzykaev^{109,c}, S. Cabrera Urbán¹⁶⁶, D. Caforio¹²⁸, V.M. Cairo^{38a,38b}, O. Cakir^{4a}, N. Calace⁵⁰, P. Calafiura¹⁵, A. Calandri⁸⁶, G. Calderini⁸¹, P. Calfayan¹⁰⁰, L.P. Caloba^{25a}, D. Calvet³⁵, S. Calvet³⁵, T.P. Calvet⁸⁶, R. Camacho Toro³², S. Camarda³¹, P. Camarri^{133a,133b}, D. Cameron¹¹⁹, R. Caminal Armadans¹⁶⁵, C. Camincher⁵⁶, S. Campana³¹, M. Campanelli⁷⁹, A. Campoverde¹⁴⁸, V. Canale^{104a,104b}, A. Canepa^{159a}, M. Cano Bret^{34e}, J. Cantero⁸³, R. Cantrill^{126a}, T. Cao⁴¹, M.D.M. Capeans Garrido³¹, I. Caprini^{27b}, M. Caprini^{27b}, M. Capua^{38a,38b}, R. Caputo⁸⁴, R.M. Carbone³⁶, R. Cardarelli^{133a}, F. Cardillo⁴⁹, T. Carli³¹, G. Carlino^{104a}, L. Carminati^{92a,92b}, S. Caron¹⁰⁶, E. Carquin^{33b}, G.D. Carrillo-Montoya³¹, J.R. Carter²⁹, J. Carvalho^{126a,126c}, D. Casadei¹⁸, M.P. Casado^{12,h}, M. Casolino¹², D.W. Casper¹⁶², E. Castaneda-Miranda^{145a}, A. Castelli¹⁰⁷, V. Castillo Gimenez¹⁶⁶, N.F. Castro^{126a,i}, A. Catinaccio³¹, J.R. Catmore¹¹⁹, A. Cattai³¹, J. Caudron⁸⁴, V. Cavaliere¹⁶⁵, E. Cavallaro¹², D. Cavalli^{92a}, M. Cavalli-Sforza¹², V. Cavasinni^{124a,124b}, F. Ceradini^{134a,134b}, L. Cerda Alberich¹⁶⁶, B.C. Cerio⁴⁶, A.S. Cerqueira^{25b}, A. Cerri¹⁴⁹, L. Cerrito⁷⁷, F. Cerutti¹⁵, M. Cerv³¹, A. Cervelli¹⁷, S.A. Cetin^{19d}, A. Chafaq^{135a}, D. Chakraborty¹⁰⁸, I. Chalupkova¹²⁹, S.K. Chan⁵⁸, Y.L. Chan^{61a}, P. Chang¹⁶⁵, J.D. Chapman²⁹, D.G. Charlton¹⁸, A. Chatterjee⁵⁰, C.C. Chau¹⁵⁸, C.A. Chavez Barajas¹⁴⁹, S. Che¹¹¹, S. Cheatham⁷³, A. Chegwiddden⁹¹, S. Chekanov⁶, S.V. Chekulaev^{159a}, G.A. Chelkov^{66,j}, M.A. Chelstowska⁹⁰, C. Chen⁶⁵, H. Chen²⁶, K. Chen¹⁴⁸, S. Chen^{34c}, S. Chen¹⁵⁵, X. Chen^{34f}, Y. Chen⁶⁸, H.C. Cheng⁹⁰, H.J. Cheng^{34a}, Y. Cheng³², A. Cheplakov⁶⁶, E. Cheremushkina¹³⁰, R. Cherkaoui El Moursli^{135e}, V. Chernyatin^{26,*}, E. Cheu⁷, L. Chevalier¹³⁶, V. Chiarella⁴⁸, G. Chiarelli^{124a,124b}, G. Chiodini^{74a}, A.S. Chisholm¹⁸, A. Chitan^{27b}, M.V. Chizhov⁶⁶, K. Choi⁶², A.R. Chomont³⁵, S. Chouridou⁹, B.K.B. Chow¹⁰⁰, V. Christodoulou⁷⁹, D. Chromek-Burckhart³¹, J. Chudoba¹²⁷, A.J. Chuinard⁸⁸, J.J. Chwastowski⁴⁰, L. Chytka¹¹⁵, G. Ciapetti^{132a,132b}, A.K. Ciftci^{4a},

D. Cinca⁵⁴, V. Cindro⁷⁶, I.A. Cioara²², A. Ciochio¹⁵, F. Ciotto^{104a,104b}, Z.H. Citron¹⁷¹, M. Ciubancan^{27b}, A. Clark⁵⁰, B.L. Clark⁵⁸, M.R. Clark³⁶, P.J. Clark⁴⁷, R.N. Clarke¹⁵, C. Clement^{146a,146b}, Y. Coadou⁸⁶, M. Cobal^{163a,163c}, A. Cocco⁵⁰, J. Cochran⁶⁵, L. Coffey²⁴, L. Colasurdo¹⁰⁶, B. Cole³⁶, S. Cole¹⁰⁸, A.P. Colijn¹⁰⁷, J. Collot⁵⁶, T. Colombo³¹, G. Compostella¹⁰¹, P. Conde Muiño^{126a,126b}, E. Coniavitis⁴⁹, S.H. Connell^{145b}, I.A. Connelly⁷⁸, V. Consorti⁴⁹, S. Constantinescu^{27b}, C. Conta^{121a,121b}, G. Conti³¹, F. Conventi^{104a,k}, M. Cooke¹⁵, B.D. Cooper⁷⁹, A.M. Cooper-Sarkar¹²⁰, T. Cornelissen¹⁷⁴, M. Corradi^{132a,132b}, F. Corriveau^{88,l}, A. Corso-Radu¹⁶², A. Cortes-Gonzalez¹², G. Cortiana¹⁰¹, G. Costa^{92a}, M.J. Costa¹⁶⁶, D. Costanzo¹³⁹, G. Cottin²⁹, G. Cowan⁷⁸, B.E. Cox⁸⁵, K. Cranmer¹¹⁰, S.J. Crawley⁵⁴, G. Cree³⁰, S. Crépé-Renaudin⁵⁶, F. Crescioli⁸¹, W.A. Cribbs^{146a,146b}, M. Crispin Ortuzar¹²⁰, M. Cristinziani²², V. Croft¹⁰⁶, G. Crosetti^{38a,38b}, T. Cuhadar Donszelmann¹³⁹, J. Cummings¹⁷⁵, M. Curatolo⁴⁸, J. Cúth⁸⁴, C. Cuthbert¹⁵⁰, H. Czirr¹⁴¹, P. Czodrowski³, S. D'Auria⁵⁴, M. D'Onofrio⁷⁵, M.J. Da Cunha Sargedas De Sousa^{126a,126b}, C. Da Via⁸⁵, W. Dabrowski^{39a}, T. Dai⁹⁰, O. Dale¹⁴, F. Dallaire⁹⁵, C. Dallapiccola⁸⁷, M. Dam³⁷, J.R. Dandoy³², N.P. Dang⁴⁹, A.C. Daniells¹⁸, N.S. Dann⁸⁵, M. Danninger¹⁶⁷, M. Dano Hoffmann¹³⁶, V. Dao⁴⁹, G. Darbo^{51a}, S. Darmora⁸, J. Dassoulas³, A. Dattagupta⁶², W. Davey²², C. David¹⁶⁸, T. Davidek¹²⁹, M. Davies¹⁵³, P. Davison⁷⁹, Y. Davygora^{59a}, E. Dawe⁸⁹, I. Dawson¹³⁹, R.K. Daya-Ishmukhametova⁸⁷, K. De⁸, R. de Asmundis^{104a}, A. De Benedetti¹¹³, S. De Castro^{21a,21b}, S. De Cecco⁸¹, N. De Groot¹⁰⁶, P. de Jong¹⁰⁷, H. De la Torre⁸³, F. De Lorenzi⁶⁵, D. De Pedis^{132a}, A. De Salvo^{132a}, U. De Sanctis¹⁴⁹, A. De Santo¹⁴⁹, J.B. De Vivie De Regie¹¹⁷, W.J. Dearnaley⁷³, R. Debbe²⁶, C. Debenedetti¹³⁷, D.V. Dedovich⁶⁶, I. Deigaard¹⁰⁷, J. Del Peso⁸³, T. Del Prete^{124a,124b}, D. Delgove¹¹⁷, F. Deliot¹³⁶, C.M. Delitzsch⁵⁰, M. Deliyergiyev⁷⁶, A. Dell'Acqua³¹, L. Dell'Asta²³, M. Dell'Orso^{124a,124b}, M. Della Pietra^{104a,k}, D. della Volpe⁵⁰, M. Delmastro⁵, P.A. Delsart⁵⁶, C. Deluca¹⁰⁷, D.A. DeMarco¹⁵⁸, S. Demers¹⁷⁵, M. Demichev⁶⁶, A. Demilly⁸¹, S.P. Denisov¹³⁰, D. Denysiuk¹³⁶, D. Derendarz⁴⁰, J.E. Derkaoui^{135d}, F. Derue⁸¹, P. Dervan⁷⁵, K. Desch²², C. Deterre⁴³, K. Dette⁴⁴, P.O. Deviveiros³¹, A. Dewhurst¹³¹, S. Dhaliwal²⁴, A. Di Ciaccio^{133a,133b}, L. Di Ciaccio⁵, W.K. Di Clemente¹²², A. Di Domenico^{132a,132b}, C. Di Donato^{132a,132b}, A. Di Girolamo³¹, B. Di Girolamo³¹, A. Di Mattia¹⁵², B. Di Micco^{134a,134b}, R. Di Nardo⁴⁸, A. Di Simone⁴⁹, R. Di Sipio¹⁵⁸, D. Di Valentino³⁰, C. Diaconu⁸⁶, M. Diamond¹⁵⁸, F.A. Dias⁴⁷, M.A. Diaz^{33a}, E.B. Diehl⁹⁰, J. Dietrich¹⁶, S. Diglio⁸⁶, A. Dimitrievska¹³, J. Dingfelder²², P. Dita^{27b}, S. Dita^{27b}, F. Dittus³¹, F. Djama⁸⁶, T. Djobava^{52b}, J.I. Djuvsland^{59a}, M.A.B. do Vale^{25c}, D. Dobos³¹, M. Dobre^{27b}, C. Doglioni⁸², T. Dohmae¹⁵⁵, J. Dolejsi¹²⁹, Z. Dolezal¹²⁹, B.A. Dolgoshein^{98,*}, M. Donadelli^{25d}, S. Donati^{124a,124b}, P. Dondero^{121a,121b}, J. Donini³⁵, J. Dopke¹³¹, A. Doria^{104a}, M.T. Dova⁷², A.T. Doyle⁵⁴, E. Drechsler⁵⁵, M. Dris¹⁰, Y. Du^{34d}, J. Duarte-Campderros¹⁵³, E. Duchovni¹⁷¹, G. Duckeck¹⁰⁰, O.A. Ducu^{27b}, D. Duda¹⁰⁷, A. Dudarev³¹, L. Duflot¹¹⁷, L. Duguid⁷⁸, M. Dührssen³¹, M. Dunford^{59a}, H. Duran Yildiz^{4a}, M. Düren⁵³, A. Durglishvili^{52b}, D. Duschinger⁴⁵, B. Dutta⁴³, M. Dyndal^{39a}, C. Eckardt⁴³, K.M. Ecker¹⁰¹, R.C. Edgar⁹⁰, W. Edson², N.C. Edwards⁴⁷, T. Eifert³¹, G. Eigen¹⁴, K. Einsweiler¹⁵, T. Ekelof¹⁶⁴, M. El Kacimi^{135c}, V. Ellajosyula⁸⁶, M. Ellert¹⁶⁴, S. Elles⁵, F. Ellinghaus¹⁷⁴, A.A. Elliot¹⁶⁸, N. Ellis³¹, J. Elmsheuser²⁶, M. Elsing³¹, D. Emelianov¹³¹, Y. Enari¹⁵⁵, O.C. Endner⁸⁴, M. Endo¹¹⁸, J.S. Ennis¹⁶⁹, J. Erdmann⁴⁴, A. Ereditato¹⁷, G. Ernis¹⁷⁴, J. Ernst², M. Ernst²⁶, S. Errede¹⁶⁵, E. Ertel⁸⁴, M. Escalier¹¹⁷, H. Esch⁴⁴, C. Escobar¹²⁵, B. Esposito⁴⁸, A.I. Etienvre¹³⁶, E. Etzion¹⁵³, H. Evans⁶², A. Ezhilov¹²³, F. Fabbri^{21a,21b}, L. Fabbri^{21a,21b}, G. Facini³², R.M. Fakhruddinov¹³⁰, S. Falciano^{132a}, R.J. Falla⁷⁹, J. Faltova¹²⁹, Y. Fang^{34a}, M. Fanti^{92a,92b}, A. Farbin⁸, A. Farilla^{134a}, C. Farina¹²⁵, T. Farooque¹², S. Farrell¹⁵, S.M. Farrington¹⁶⁹, P. Farthouat³¹, F. Fassi^{135e}, P. Fassnacht³¹, D. Fassoulotis⁹, M. Fauci Giannelli⁷⁸, A. Favareto^{51a,51b}, W.J. Fawcett¹²⁰, L. Fayard¹¹⁷, O.L. Fedin^{123,m}, W. Fedorko¹⁶⁷, S. Feigl¹¹⁹, L. Feligioni⁸⁶, C. Feng^{34d}, E.J. Feng³¹, H. Feng⁹⁰, A.B. Fenyuk¹³⁰, L. Feremenga⁸, P. Fernandez Martinez¹⁶⁶, S. Fernandez Perez¹², J. Ferrando⁵⁴, A. Ferrari¹⁶⁴, P. Ferrari¹⁰⁷, R. Ferrari^{121a}, D.E. Ferreira de Lima⁵⁴, A. Ferrer¹⁶⁶, D. Ferrere⁵⁰, C. Ferretti⁹⁰, A. Ferretto Parodi^{51a,51b}, F. Fiedler⁸⁴, A. Filipčič⁷⁶, M. Filipuzzi⁴³, F. Filthaut¹⁰⁶, M. Fincke-Keeler¹⁶⁸, K.D. Finelli¹⁵⁰, M.C.N. Fiolhais^{126a,126c}, L. Fiorini¹⁶⁶, A. Firan⁴¹, A. Fischer², C. Fischer¹², J. Fischer¹⁷⁴, W.C. Fisher⁹¹, N. Flaschel⁴³, I. Fleck¹⁴¹, P. Fleischmann⁹⁰, G.T. Fletcher¹³⁹, G. Fletcher⁷⁷, R.R.M. Fletcher¹²², T. Flick¹⁷⁴, A. Floderus⁸², L.R. Flores Castillo^{61a}, M.J. Flowerdew¹⁰¹, G.T. Forcolin⁸⁵, A. Formica¹³⁶, A. Forti⁸⁵, A.G. Foster¹⁸, D. Fournier¹¹⁷, H. Fox⁷³, S. Fracchia¹², P. Francavilla⁸¹, M. Franchini^{21a,21b}, D. Francis³¹, L. Franconi¹¹⁹, M. Franklin⁵⁸, M. Frate¹⁶², M. Fraternali^{121a,121b}, D. Freeborn⁷⁹, S.M. Fressard-Batraneanu³¹, F. Friedrich⁴⁵,

D. Froidevaux³¹, J.A. Frost¹²⁰, C. Fukunaga¹⁵⁶, E. Fullana Torregrosa⁸⁴, T. Fusayasu¹⁰², J. Fuster¹⁶⁶, C. Gabaldon⁵⁶, O. Gabizon¹⁷⁴, A. Gabrielli^{21a,21b}, A. Gabrielli¹⁵, G.P. Gach^{39a}, S. Gadatsch³¹, S. Gadowski⁵⁰, G. Gagliardi^{51a,51b}, L.G. Gagnon⁹⁵, P. Gagnon⁶², C. Galea¹⁰⁶, B. Galhardo^{126a,126c}, E.J. Gallas¹²⁰, B.J. Gallop¹³¹, P. Gallus¹²⁸, G. Galster³⁷, K.K. Gan¹¹¹, J. Gao^{34b,86}, Y. Gao⁴⁷, Y.S. Gao^{143,f}, F.M. Garay Walls⁴⁷, C. García¹⁶⁶, J.E. García Navarro¹⁶⁶, M. Garcia-Sciveres¹⁵, R.W. Gardner³², N. Garelli¹⁴³, V. Garonne¹¹⁹, A. Gascon Bravo⁴³, C. Gatti⁴⁸, A. Gaudiello^{51a,51b}, G. Gaudio^{121a}, B. Gaur¹⁴¹, L. Gauthier⁹⁵, I.L. Gavrilenko⁹⁶, C. Gay¹⁶⁷, G. Gaycken²², E.N. Gazis¹⁰, Z. Gecse¹⁶⁷, C.N.P. Gee¹³¹, Ch. Geich-Gimbel²², M.P. Geisler^{59a}, C. Gemme^{51a}, M.H. Genest⁵⁶, C. Geng^{34b,n}, S. Gentile^{132a,132b}, S. George⁷⁸, D. Gerbaudo¹⁶², A. Gershon¹⁵³, S. Ghasemi¹⁴¹, H. Ghazlane^{135b}, M. Ghneimat²², B. Giacobbe^{21a}, S. Giagu^{132a,132b}, P. Giannetti^{124a,124b}, B. Gibbard²⁶, S.M. Gibson⁷⁸, M. Gignac¹⁶⁷, M. Gilchriese¹⁵, T.P.S. Gillam²⁹, D. Gillberg³⁰, G. Gilles¹⁷⁴, D.M. Gingrich^{3,d}, N. Giokaris⁹, M.P. Giordani^{163a,163c}, F.M. Giorgi^{21a}, F.M. Giorgi¹⁶, P.F. Giraud¹³⁶, P. Giromini⁵⁸, D. Giugni^{92a}, F. Giuli¹²⁰, C. Giuliani¹⁰¹, M. Giulini^{59b}, B.K. Gjelsten¹¹⁹, S. Gkaitatzis¹⁵⁴, I. Gkialas¹⁵⁴, E.L. Gkougkousis¹¹⁷, L.K. Gladilin⁹⁹, C. Glasman⁸³, J. Glatzer³¹, P.C.F. Glaysheer⁴⁷, A. Glazov⁴³, M. Goblirsch-Kolb¹⁰¹, J. Godlewski⁴⁰, S. Goldfarb⁹⁰, T. Golling⁵⁰, D. Golubkov¹³⁰, A. Gomes^{126a,126b,126d}, R. Gonçalves^{126a}, J. Goncalves Pinto Firmino Da Costa¹³⁶, L. Gonella¹⁸, A. Gongadze⁶⁶, S. González de la Hoz¹⁶⁶, G. Gonzalez Parra¹², S. Gonzalez-Sevilla⁵⁰, L. Goossens³¹, P.A. Gorbounov⁹⁷, H.A. Gordon²⁶, I. Gorelov¹⁰⁵, B. Gorini³¹, E. Gorini^{74a,74b}, A. Gorišek⁷⁶, E. Gornicki⁴⁰, A.T. Goshaw⁴⁶, C. Gössling⁴⁴, M.I. Gostkin⁶⁶, C.R. Goudet¹¹⁷, D. Goujdami^{135c}, A.G. Goussiou¹³⁸, N. Govender^{145b}, E. Gozani¹⁵², L. Graber⁵⁵, I. Grabowska-Bold^{39a}, P.O.J. Gradin¹⁶⁴, P. Grafström^{21a,21b}, J. Gramling⁵⁰, E. Gramstad¹¹⁹, S. Grancagnolo¹⁶, V. Gratchev¹²³, H.M. Gray³¹, E. Graziani^{134a}, Z.D. Greenwood^{80,o}, C. Grefe²², K. Gregersen⁷⁹, I.M. Gregor⁴³, P. Grenier¹⁴³, K. Grevtsov⁵, J. Griffiths⁸, A.A. Grillo¹³⁷, K. Grimm⁷³, S. Grinstein^{12,p}, Ph. Gris³⁵, J.-F. Grivaz¹¹⁷, S. Groh⁸⁴, J.P. Grohs⁴⁵, E. Gross¹⁷¹, J. Grosse-Knetter⁵⁵, G.C. Grossi⁸⁰, Z.J. Grout¹⁴⁹, L. Guan⁹⁰, W. Guan¹⁷², J. Guenther¹²⁸, F. Guescini⁵⁰, D. Guest¹⁶², O. Gueta¹⁵³, E. Guido^{51a,51b}, T. Guillemain⁵, S. Guindon², U. Gul⁵⁴, C. Gumpert³¹, J. Guo^{34e}, Y. Guo^{34b,n}, S. Gupta¹²⁰, G. Gustavino^{132a,132b}, P. Gutierrez¹¹³, N.G. Gutierrez Ortiz⁷⁹, C. Gutsche⁴⁵, C. Guyot¹³⁶, C. Gwenlan¹²⁰, C.B. Gwilliam⁷⁵, A. Haas¹¹⁰, C. Haber¹⁵, H.K. Hadavand⁸, N. Haddad^{135e}, A. Hadeef⁸⁶, P. Haefner²², S. Hageböck²², Z. Hajduk⁴⁰, H. Hakobyan^{176,*}, M. Haleem⁴³, J. Haley¹¹⁴, D. Hall¹²⁰, G. Halladjian⁹¹, G.D. Hallewell⁸⁶, K. Hamacher¹⁷⁴, P. Hamal¹¹⁵, K. Hamano¹⁶⁸, A. Hamilton^{145a}, G.N. Hamity¹³⁹, P.G. Hamnett⁴³, L. Han^{34b}, K. Hanagaki^{67,q}, K. Hanawa¹⁵⁵, M. Hance¹³⁷, B. Haney¹²², P. Hanke^{59a}, R. Hanna¹³⁶, J.B. Hansen³⁷, J.D. Hansen³⁷, M.C. Hansen²², P.H. Hansen³⁷, K. Hara¹⁶⁰, A.S. Hard¹⁷², T. Harenberg¹⁷⁴, F. Hariri¹¹⁷, S. Harkusha⁹³, R.D. Harrington⁴⁷, P.F. Harrison¹⁶⁹, F. Hartjes¹⁰⁷, M. Hasegawa⁶⁸, Y. Hasegawa¹⁴⁰, A. Hasib¹¹³, S. Hassani¹³⁶, S. Haug¹⁷, R. Hauser⁹¹, L. Hauswald⁴⁵, M. Havranek¹²⁷, C.M. Hawkes¹⁸, R.J. Hawkings³¹, A.D. Hawkins⁸², D. Hayden⁹¹, C.P. Hays¹²⁰, J.M. Hays⁷⁷, H.S. Hayward⁷⁵, S.J. Haywood¹³¹, S.J. Head¹⁸, T. Heck⁸⁴, V. Hedberg⁸², L. Heelan⁸, S. Heim¹²², T. Heim¹⁵, B. Heinemann¹⁵, J.J. Heinrich¹⁰⁰, L. Heinrich¹¹⁰, C. Heinz⁵³, J. Hejbal¹²⁷, L. Helary²³, S. Hellman^{146a,146b}, C. Hensens³¹, J. Henderson¹²⁰, R.C.W. Henderson⁷³, Y. Heng¹⁷², S. Henkelmann¹⁶⁷, A.M. Henriques Correia³¹, S. Henrot-Versille¹¹⁷, G.H. Herbert¹⁶, Y. Hernández Jiménez¹⁶⁶, G. Herten⁴⁹, R. Hertenberger¹⁰⁰, L. Hervas³¹, G.G. Hesketh⁷⁹, N.P. Hessey¹⁰⁷, J.W. Hetherly⁴¹, R. Hickling⁷⁷, E. Higón-Rodríguez¹⁶⁶, E. Hill¹⁶⁸, J.C. Hill²⁹, K.H. Hiller⁴³, S.J. Hillier¹⁸, I. Hinchliffe¹⁵, E. Hines¹²², R.R. Hinman¹⁵, M. Hirose¹⁵⁷, D. Hirschbuehl¹⁷⁴, J. Hobbs¹⁴⁸, N. Hod¹⁰⁷, M.C. Hodgkinson¹³⁹, P. Hodgson¹³⁹, A. Hoecker³¹, M.R. Hoefkamp¹⁰⁵, F. Hoenig¹⁰⁰, M. Hohlfeld⁸⁴, D. Hohn²², T.R. Holmes¹⁵, M. Homann⁴⁴, T.M. Hong¹²⁵, B.H. Hooberman¹⁶⁵, W.H. Hopkins¹¹⁶, Y. Horii¹⁰³, A.J. Horton¹⁴², J.-Y. Hostachy⁵⁶, S. Hou¹⁵¹, A. Hoummada^{135a}, J. Howard¹²⁰, J. Howarth⁴³, M. Hrabovsky¹¹⁵, I. Hristova¹⁶, J. Hrivnac¹¹⁷, T. Hryn'ova⁵, A. Hrynevich⁹⁴, C. Hsu^{145c}, P.J. Hsu^{151,r}, S.-C. Hsu¹³⁸, D. Hu³⁶, Q. Hu^{34b}, Y. Huang⁴³, Z. Hubacek¹²⁸, F. Hubaut⁸⁶, F. Huegging²², T.B. Huffman¹²⁰, E.W. Hughes³⁶, G. Hughes⁷³, M. Huhtinen³¹, T.A. Hülsing⁸⁴, N. Huseynov^{66,b}, J. Huston⁹¹, J. Huth⁵⁸, G. Iacobucci⁵⁰, G. Iakovidis²⁶, I. Ibragimov¹⁴¹, L. Iconomidou-Fayard¹¹⁷, E. Ideal¹⁷⁵, Z. Idrissi^{135e}, P. Iengo³¹, O. Igonkina¹⁰⁷, T. Iizawa¹⁷⁰, Y. Ikegami⁶⁷, M. Ikeno⁶⁷, Y. Ilchenko^{32,s}, D. Iliadis¹⁵⁴, N. Ilic¹⁴³, T. Ince¹⁰¹, G. Introzzi^{121a,121b}, P. Ioannou^{9,*}, M. Iodice^{134a}, K. Iordanidou³⁶, V. Ippolito⁵⁸, A. Irles Quiles¹⁶⁶, C. Isaksson¹⁶⁴, M. Ishino⁶⁹, M. Ishitsuka¹⁵⁷,

R. Ishmukhametov¹¹¹, C. Issever¹²⁰, S. Istin^{19a}, F. Ito¹⁶⁰, J.M. Iturbe Ponce⁸⁵, R. Iuppa^{133a,133b}, J. Ivarsson⁸², W. Iwanski⁴⁰, H. Iwasaki⁶⁷, J.M. Izen⁴², V. Izzo^{104a}, S. Jabbar³, B. Jackson¹²², M. Jackson⁷⁵, P. Jackson¹, V. Jain², K.B. Jakobi⁸⁴, K. Jakobs⁴⁹, S. Jakobsen³¹, T. Jakoubek¹²⁷, D.O. Jamin¹¹⁴, D.K. Jana⁸⁰, E. Jansen⁷⁹, R. Jansky⁶³, J. Janssen²², M. Janus⁵⁵, G. Jarlskog⁸², N. Javadov^{66,b}, T. Javůrek⁴⁹, F. Jeanneau¹³⁶, L. Jeanty¹⁵, J. Jejelava^{52a,t}, G.-Y. Jeng¹⁵⁰, D. Jennens⁸⁹, P. Jenni^{49,u}, J. Jentzsch⁴⁴, C. Jeske¹⁶⁹, S. Jézéquel⁵, H. Ji¹⁷², J. Jia¹⁴⁸, H. Jiang⁶⁵, Y. Jiang^{34b}, S. Jiggins⁷⁹, J. Jimenez Pena¹⁶⁶, S. Jin^{34a}, A. Jinaru^{27b}, O. Jinnouchi¹⁵⁷, P. Johansson¹³⁹, K.A. Johns⁷, W.J. Johnson¹³⁸, K. Jon-And^{146a,146b}, G. Jones¹⁶⁹, R.W.L. Jones⁷³, S. Jones⁷, T.J. Jones⁷⁵, J. Jongmanns^{59a}, P.M. Jorge^{126a,126b}, J. Jovicevic^{159a}, X. Ju¹⁷², A. Juste Rozas^{12,p}, M.K. Köhler¹⁷¹, A. Kaczmarek⁴⁰, M. Kado¹¹⁷, H. Kagan¹¹¹, M. Kagan¹⁴³, S.J. Kahn⁸⁶, E. Kajomovitz⁴⁶, C.W. Kalderon¹²⁰, A. Kaluza⁸⁴, S. Kama⁴¹, A. Kamenshchikov¹³⁰, N. Kanaya¹⁵⁵, S. Kaneti²⁹, L. Kanjir⁷⁶, V.A. Kantserov⁹⁸, J. Kanzaki⁶⁷, B. Kaplan¹¹⁰, L.S. Kaplan¹⁷², A. Kapliy³², D. Kar^{145c}, K. Karakostas¹⁰, A. Karamaoun³, N. Karastathis¹⁰, M.J. Kareem⁵⁵, E. Karentzos¹⁰, M. Karnevskiy⁸⁴, S.N. Karpov⁶⁶, Z.M. Karpova⁶⁶, K. Karthik¹¹⁰, V. Kartvelishvili⁷³, A.N. Karyukhin¹³⁰, K. Kasahara¹⁶⁰, L. Kashif¹⁷², R.D. Kass¹¹¹, A. Kastanas¹⁴, Y. Kataoka¹⁵⁵, C. Kato¹⁵⁵, A. Katre⁵⁰, J. Katzy⁴³, K. Kawade¹⁰³, K. Kawagoe⁷¹, T. Kawamoto¹⁵⁵, G. Kawamura⁵⁵, S. Kazama¹⁵⁵, V.F. Kazanin^{109,c}, R. Keeler¹⁶⁸, R. Kehoe⁴¹, J.S. Keller⁴³, J.J. Kempster⁷⁸, H. Keoshkerian⁸⁵, O. Kepka¹²⁷, B.P. Kerševan⁷⁶, S. Kersten¹⁷⁴, R.A. Keyes⁸⁸, F. Khalil-zada¹¹, H. Khandanyan^{146a,146b}, A. Khanov¹¹⁴, A.G. Kharlamov^{109,c}, T.J. Khoo²⁹, V. Khovanskiy⁹⁷, E. Khramov⁶⁶, J. Khubua^{52b,v}, S. Kido⁶⁸, H.Y. Kim⁸, S.H. Kim¹⁶⁰, Y.K. Kim³², N. Kimura¹⁵⁴, O.M. Kind¹⁶, B.T. King⁷⁵, M. King¹⁶⁶, S.B. King¹⁶⁷, J. Kirk¹³¹, A.E. Kiryunin¹⁰¹, T. Kishimoto⁶⁸, D. Kisielewska^{39a}, F. Kiss⁴⁹, K. Kiuchi¹⁶⁰, O. Kivernyk¹³⁶, E. Kladiva^{144b}, M.H. Klein³⁶, M. Klein⁷⁵, U. Klein⁷⁵, K. Kleinknecht⁸⁴, P. Klimek^{146a,146b}, A. Klimentov²⁶, R. Klingenberg⁴⁴, J.A. Klinger¹³⁹, T. Klioutchnikova³¹, E.-E. Kluge^{59a}, P. Kluit¹⁰⁷, S. Kluth¹⁰¹, J. Knapik⁴⁰, E. Kneringer⁶³, E.B.F.G. Knoops⁸⁶, A. Knue⁵⁴, A. Kobayashi¹⁵⁵, D. Kobayashi¹⁵⁷, T. Kobayashi¹⁵⁵, M. Kobel⁴⁵, M. Kocian¹⁴³, P. Kodys¹²⁹, T. Koffas³⁰, E. Koffeman¹⁰⁷, L.A. Kogan¹²⁰, T. Kohriki⁶⁷, T. Koi¹⁴³, H. Kolanoski¹⁶, M. Kolb^{59b}, I. Koletsou⁵, A.A. Komar^{96,*}, Y. Komori¹⁵⁵, T. Kondo⁶⁷, N. Kondrashova⁴³, K. Köneke⁴⁹, A.C. König¹⁰⁶, T. Kono^{67,w}, R. Konoplich^{110,x}, N. Konstantinidis⁷⁹, R. Kopeliansky⁶², S. Koperny^{39a}, L. Köpke⁸⁴, A.K. Kopp⁴⁹, K. Korcyl⁴⁰, K. Kordas¹⁵⁴, A. Korn⁷⁹, A.A. Korol^{109,c}, I. Korolkov¹², E.V. Korolkova¹³⁹, O. Kortner¹⁰¹, S. Kortner¹⁰¹, T. Kosek¹²⁹, V.V. Kostyukhin²², V.M. Kotov⁶⁶, A. Kotwal⁴⁶, A. Kourkouveli-Charalampidi¹⁵⁴, C. Kourkouvelis⁹, V. Kouskoura²⁶, A. Koutsman^{159a}, A.B. Kowalewska⁴⁰, R. Kowalewski¹⁶⁸, T.Z. Kowalski^{39a}, W. Kozanecki¹³⁶, A.S. Kozhin¹³⁰, V.A. Kramarenko⁹⁹, G. Kramberger⁷⁶, D. Krasnopevtsev⁹⁸, M.W. Krasny⁸¹, A. Krasznahorkay³¹, J.K. Kraus²², A. Kravchenko²⁶, M. Kretz^{59c}, J. Kretzschmar⁷⁵, K. Kreutzfeldt⁵³, P. Krieger¹⁵⁸, K. Krizka³², K. Kroeninger⁴⁴, H. Kroha¹⁰¹, J. Kroll¹²², J. Kroseberg²², J. Krstic¹³, U. Kruchonak⁶⁶, H. Krüger²², N. Krumnack⁶⁵, A. Kruse¹⁷², M.C. Kruse⁴⁶, M. Kruskal²³, T. Kubota⁸⁹, H. Kucuk⁷⁹, S. Kuday^{4b}, J.T. Kuechler¹⁷⁴, S. Kuehn⁴⁹, A. Kugel^{59c}, F. Kuger¹⁷³, A. Kuhl¹³⁷, T. Kuhl⁴³, V. Kukhtin⁶⁶, R. Kukla¹³⁶, Y. Kulchitsky⁹³, S. Kuleshov^{33b}, M. Kuna^{132a,132b}, T. Kunigo⁶⁹, A. Kupco¹²⁷, H. Kurashige⁶⁸, Y.A. Kurochkin⁹³, V. Kus¹²⁷, E.S. Kuwertz¹⁶⁸, M. Kuze¹⁵⁷, J. Kvita¹¹⁵, T. Kwan¹⁶⁸, D. Kyriazopoulos¹³⁹, A. La Rosa¹⁰¹, J.L. La Rosa Navarro^{25d}, L. La Rotonda^{38a,38b}, C. Lacasta¹⁶⁶, F. Lacava^{132a,132b}, J. Lacey³⁰, H. Lacker¹⁶, D. Lacour⁸¹, V.R. Lacuesta¹⁶⁶, E. Ladygin⁶⁶, R. Lafaye⁵, B. Laforge⁸¹, T. Lagouri¹⁷⁵, S. Lai⁵⁵, S. Lammers⁶², W. Lampl⁷, E. Lançon¹³⁶, U. Landgraf⁴⁹, M.P.J. Landon⁷⁷, V.S. Lang^{59a}, J.C. Lange¹², A.J. Lankford¹⁶², F. Lanni²⁶, K. Lantzsche²², A. Lanza^{121a}, S. Laplace⁸¹, C. Lapoire³¹, J.F. Laporte¹³⁶, T. Lari^{92a}, F. Lasagni Manghi^{21a,21b}, M. Lassnig³¹, P. Laurelli⁴⁸, W. Lavrijsen¹⁵, A.T. Law¹³⁷, P. Laycock⁷⁵, T. Lazovich⁵⁸, M. Lazzaroni^{92a,92b}, O. Le Dortz⁸¹, E. Le Guirriec⁸⁶, E. Le Menedeu¹², E.P. Le Quilleuc¹³⁶, M. LeBlanc¹⁶⁸, T. LeCompte⁶, F. Ledroit-Guillon⁵⁶, C.A. Lee²⁶, S.C. Lee¹⁵¹, L. Lee¹, G. Lefebvre⁸¹, M. Lefebvre¹⁶⁸, F. Legger¹⁰⁰, C. Leggett¹⁵, A. Lehan⁷⁵, G. Lehmann Miotto³¹, X. Lei⁷, W.A. Leight³⁰, A. Leisos^{154,y}, A.G. Leister¹⁷⁵, M.A.L. Leite^{25d}, R. Leitner¹²⁹, D. Lellouch¹⁷¹, B. Lemmer⁵⁵, K.J.C. Leney⁷⁹, T. Lenz²², B. Lenzi³¹, R. Leone⁷, S. Leone^{124a,124b}, C. Leonidopoulos⁴⁷, S. Leontsinis¹⁰, G. Lerner¹⁴⁹, C. Leroy⁹⁵, A.A.J. Lesage¹³⁶, C.G. Lester²⁹, M. Levchenko¹²³, J. Levêque⁵, D. Levin⁹⁰, L.J. Levinson¹⁷¹, M. Levy¹⁸, A.M. Leyko²², M. Leyton⁴², B. Li^{34b,z}, H. Li¹⁴⁸, H.L. Li³², L. Li⁴⁶, L. Li^{34e}, Q. Li^{34a}, S. Li⁴⁶, X. Li⁸⁵, Y. Li¹⁴¹, Z. Liang¹³⁷, H. Liao³⁵, B. Liberti^{133a}, A. Liblong¹⁵⁸, P. Lichard³¹, K. Lie¹⁶⁵, J. Liebal²², W. Liebig¹⁴, C. Limbach²², A. Limosani¹⁵⁰, S.C. Lin^{151,aa}, T.H. Lin⁸⁴, B.E. Lindquist¹⁴⁸, E. Lipeles¹²², A. Lipniacka¹⁴, M. Lisovsky^{59b},

T.M. Liss¹⁶⁵, D. Lissauer²⁶, A. Lister¹⁶⁷, A.M. Litke¹³⁷, B. Liu^{151,ab}, D. Liu¹⁵¹, H. Liu⁹⁰, H. Liu²⁶, J. Liu⁸⁶, J.B. Liu^{34b}, K. Liu⁸⁶, L. Liu¹⁶⁵, M. Liu⁴⁶, M. Liu^{34b}, Y.L. Liu^{34b}, Y. Liu^{34b}, M. Livan^{121a,121b}, A. Lleres⁵⁶, J. Llorente Merino⁸³, S.L. Lloyd⁷⁷, F. Lo Sterzo¹⁵¹, E. Lobodzinska⁴³, P. Loch⁷, W.S. Lockman¹³⁷, F.K. Loebinger⁸⁵, A.E. Loevschall-Jensen³⁷, K.M. Loew²⁴, A. Loginov¹⁷⁵, T. Lohse¹⁶, K. Lohwasser⁴³, M. Lokajicek¹²⁷, B.A. Long²³, J.D. Long¹⁶⁵, R.E. Long⁷³, L. Longo^{74a,74b}, K.A. Looper¹¹¹, L. Lopes^{126a}, D. Lopez Mateos⁵⁸, B. Lopez Paredes¹³⁹, I. Lopez Paz¹², A. Lopez Solis⁸¹, J. Lorenz¹⁰⁰, N. Lorenzo Martinez⁶², M. Losada²⁰, P.J. Lösel¹⁰⁰, X. Lou^{34a}, A. Lounis¹¹⁷, J. Love⁶, P.A. Love⁷³, H. Lu^{61a}, N. Lu⁹⁰, H.J. Lubatti¹³⁸, C. Luci^{132a,132b}, A. Lucotte⁵⁶, C. Luedtke⁴⁹, F. Luehring⁶², W. Lukas⁶³, L. Luminari^{132a}, O. Lundberg^{146a,146b}, B. Lund-Jensen¹⁴⁷, D. Lynn²⁶, R. Lysak¹²⁷, E. Lytken⁸², V. Lyubushkin⁶⁶, H. Ma²⁶, L.L. Ma^{34d}, Y. Ma^{34d}, G. Maccarrone⁴⁸, A. Macchiolo¹⁰¹, C.M. Macdonald¹³⁹, B. Maček⁷⁶, J. Machado Miguens^{122,126b}, D. Madaffari⁸⁶, R. Madar³⁵, H.J. Maddocks¹⁶⁴, W.F. Mader⁴⁵, A. Madsen⁴³, J. Maeda⁶⁸, S. Maeland¹⁴, T. Maeno²⁶, A. Maevskiy⁹⁹, E. Magradze⁵⁵, J. Mahlstedt¹⁰⁷, C. Maiani¹¹⁷, C. Maidantchik^{25a}, A.A. Maier¹⁰¹, T. Maier¹⁰⁰, A. Maio^{126a,126b,126d}, S. Majewski¹¹⁶, Y. Makida⁶⁷, N. Makovec¹¹⁷, B. Malaescu⁸¹, Pa. Malecki⁴⁰, V.P. Maleev¹²³, F. Malek⁵⁶, U. Mallik⁶⁴, D. Malon⁶, C. Malone¹⁴³, S. Maltezos¹⁰, V.M. Malyshev¹⁰⁹, S. Malyukov³¹, J. Mamuzic⁴³, G. Mancini⁴⁸, B. Mandelli³¹, L. Mandelli^{92a}, I. Mandić⁷⁶, J. Maneira^{126a,126b}, L. Manhaes de Andrade Filho^{25b}, J. Manjarres Ramos^{159b}, A. Mann¹⁰⁰, B. Mansoulie¹³⁶, R. Mantifel⁸⁸, M. Mantoani⁵⁵, S. Manzoni^{92a,92b}, L. Mapelli³¹, G. Marceca²⁸, L. March⁵⁰, G. Marchiori⁸¹, M. Marcisovsky¹²⁷, M. Marjanovic¹³, D.E. Marley⁹⁰, F. Marroquim^{25a}, S.P. Marsden⁸⁵, Z. Marshall¹⁵, L.F. Marti¹⁷, S. Marti-Garcia¹⁶⁶, B. Martin⁹¹, T.A. Martin¹⁶⁹, V.J. Martin⁴⁷, B. Martin dit Latour¹⁴, M. Martinez^{12,p}, S. Martin-Haugh¹³¹, V.S. Martoiu^{27b}, A.C. Martyniuk⁷⁹, M. Marx¹³⁸, F. Marzano^{132a}, A. Marzin³¹, L. Masetti⁸⁴, T. Mashimo¹⁵⁵, R. Mashinistov⁹⁶, J. Masik⁸⁵, A.L. Maslennikov^{109,c}, I. Massa^{21a,21b}, L. Massa^{21a,21b}, P. Mastrandrea⁵, A. Mastroberardino^{38a,38b}, T. Masubuchi¹⁵⁵, P. Mättig¹⁷⁴, J. Mattmann⁸⁴, J. Maurer^{27b}, S.J. Maxfield⁷⁵, D.A. Maximov^{109,c}, R. Mazini¹⁵¹, S.M. Mazza^{92a,92b}, N.C. Mc Fadden¹⁰⁵, G. Mc Goldrick¹⁵⁸, S.P. Mc Kee⁹⁰, A. McCarn⁹⁰, R.L. McCarthy¹⁴⁸, T.G. McCarthy³⁰, L.I. McClymont⁷⁹, K.W. McFarlane^{57,*}, J.A. Mcfayden⁷⁹, G. Mchedlidze⁵⁵, S.J. McMahon¹³¹, R.A. McPherson^{168,l}, M. Medinnis⁴³, S. Meehan¹³⁸, S. Mehlhase¹⁰⁰, A. Mehta⁷⁵, K. Meier^{59a}, C. Meineck¹⁰⁰, B. Meirose⁴², B.R. Mellado Garcia^{145c}, F. Meloni¹⁷, A. Mengarelli^{21a,21b}, S. Menke¹⁰¹, E. Meoni¹⁶¹, K.M. Mercurio⁵⁸, S. Mergelmeyer¹⁶, P. Mermod⁵⁰, L. Merola^{104a,104b}, C. Meroni^{92a}, F.S. Merritt³², A. Messina^{132a,132b}, J. Metcalfe⁶, A.S. Mete¹⁶², C. Meyer⁸⁴, C. Meyer¹²², J-P. Meyer¹³⁶, J. Meyer¹⁰⁷, H. Meyer Zu Theenhausen^{59a}, R.P. Middleton¹³¹, S. Miglioranza^{163a,163c}, L. Mijović²², G. Mikenberg¹⁷¹, M. Mikestikova¹²⁷, M. Mikuž⁷⁶, M. Milesi⁸⁹, A. Milic³¹, D.W. Miller³², C. Mills⁴⁷, A. Milov¹⁷¹, D.A. Milstead^{146a,146b}, A.A. Minaenko¹³⁰, Y. Minami¹⁵⁵, I.A. Minashvili⁶⁶, A.I. Mincer¹¹⁰, B. Mindur^{39a}, M. Mineev⁶⁶, Y. Ming¹⁷², L.M. Mir¹², K.P. Mistry¹²², T. Mitani¹⁷⁰, J. Mitrevski¹⁰⁰, V.A. Mitsou¹⁶⁶, A. Miucci⁵⁰, P.S. Miyagawa¹³⁹, J.U. Mjörnmark⁸², T. Moa^{146a,146b}, K. Mochizuki⁸⁶, S. Mohapatra³⁶, W. Mohr⁴⁹, S. Molander^{146a,146b}, R. Moles-Valls²², R. Monden⁶⁹, M.C. Mondragon⁹¹, K. Mönig⁴³, J. Monk³⁷, E. Monnier⁸⁶, A. Montalbano¹⁴⁸, J. Montejo Berlingen³¹, F. Monticelli⁷², S. Monzani^{92a,92b}, R.W. Moore³, N. Morange¹¹⁷, D. Moreno²⁰, M. Moreno Llacer⁵⁵, P. Morettini^{51a}, D. Mori¹⁴², T. Mori¹⁵⁵, M. Morii⁵⁸, M. Morinaga¹⁵⁵, V. Morisbak¹¹⁹, S. Moritz⁸⁴, A.K. Morley¹⁵⁰, G. Mornacchi³¹, J.D. Morris⁷⁷, S.S. Mortensen³⁷, L. Morvaj¹⁴⁸, M. Mosidze^{52b}, J. Moss¹⁴³, K. Motohashi¹⁵⁷, R. Mount¹⁴³, E. Mountricha²⁶, S.V. Mouraviev^{96,*}, E.J.W. Moyse⁸⁷, S. Muanza⁸⁶, R.D. Mudd¹⁸, F. Mueller¹⁰¹, J. Mueller¹²⁵, R.S.P. Mueller¹⁰⁰, T. Mueller²⁹, D. Muenstermann⁷³, P. Mullen⁵⁴, G.A. Mullier¹⁷, F.J. Munoz Sanchez⁸⁵, J.A. Murillo Quijada¹⁸, W.J. Murray^{169,131}, H. Musheghyan⁵⁵, M. Muskinja⁷⁶, A.G. Myagkov^{130,ac}, M. Myska¹²⁸, B.P. Nachman¹⁴³, O. Nackenhorst⁵⁰, J. Nadal⁵⁵, K. Nagai¹²⁰, R. Nagai^{67,w}, K. Nagano⁶⁷, Y. Nagasaka⁶⁰, K. Nagata¹⁶⁰, M. Nagel¹⁰¹, E. Nagy⁸⁶, A.M. Nairz³¹, Y. Nakahama³¹, K. Nakamura⁶⁷, T. Nakamura¹⁵⁵, I. Nakano¹¹², H. Namasivayam⁴², R.F. Naranjo Garcia⁴³, R. Narayan³², D.I. Narrias Villar^{59a}, I. Naryshkin¹²³, T. Naumann⁴³, G. Navarro²⁰, R. Nayyar⁷, H.A. Neal⁹⁰, P.Yu. Nechaeva⁹⁶, F. Nechansky¹²⁷, T.J. Neep⁸⁵, P.D. Nef¹⁴³, A. Negri^{121a,121b}, M. Negrini^{21a}, S. Nektarijevic¹⁰⁶, C. Nellist¹¹⁷, A. Nelson¹⁶², S. Nemecek¹²⁷, P. Nemethy¹¹⁰, A.A. Nepomuceno^{25a}, M. Nessi^{31,ad}, M.S. Neubauer¹⁶⁵, M. Neumann¹⁷⁴, R.M. Neves¹¹⁰, P. Nevski²⁶, P.R. Newman¹⁸, D.H. Nguyen⁶, R.B. Nickerson¹²⁰, R. Nicolaïdou¹³⁶, B. Nicquevert³¹, J. Nielsen¹³⁷, A. Nikiforov¹⁶, V. Nikolaenko^{130,ac}, I. Nikolic-Audit⁸¹, K. Nikolopoulos¹⁸, J.K. Nilsen¹¹⁹, P. Nilsson²⁶,

Y. Ninomiya¹⁵⁵, A. Nisati^{132a}, R. Nisius¹⁰¹, T. Nobe¹⁵⁵, L. Nodulman⁶, M. Nomachi¹¹⁸, I. Nomidis³⁰, T. Nooney⁷⁷, S. Norberg¹¹³, M. Nordberg³¹, N. Norjoharuddeen¹²⁰, O. Novgorodova⁴⁵, S. Nowak¹⁰¹, M. Nozaki⁶⁷, L. Nozka¹¹⁵, K. Ntekas¹⁰, E. Nurse⁷⁹, F. Nuti⁸⁹, F. O'grady⁷, D.C. O'Neil¹⁴², A.A. O'Rourke⁴³, V. O'Shea⁵⁴, F.G. Oakham^{30,d}, H. Oberlack¹⁰¹, T. Obermann²², J. Ocariz⁸¹, A. Ochi⁶⁸, I. Ochoa³⁶, J.P. Ochoa-Ricoux^{33a}, S. Oda⁷¹, S. Odaka⁶⁷, H. Ogren⁶², A. Oh⁸⁵, S.H. Oh⁴⁶, C.C. Ohm¹⁵, H. Ohman¹⁶⁴, H. Oide³¹, H. Okawa¹⁶⁰, Y. Okumura³², T. Okuyama⁶⁷, A. Olariu^{27b}, L.F. Oleiro Seabra^{126a}, S.A. Olivares Pino⁴⁷, D. Oliveira Damazio²⁶, A. Olszewski⁴⁰, J. Olszowska⁴⁰, A. Onofre^{126a,126e}, K. Onogi¹⁰³, P.U.E. Onyisi^{32,s}, C.J. Oram^{159a}, M.J. Oreglia³², Y. Oren¹⁵³, D. Orestano^{134a,134b}, N. Orlando^{61b}, R.S. Orr¹⁵⁸, B. Osculati^{51a,51b}, R. Ospanov⁸⁵, G. Otero y Garzon²⁸, H. Otono⁷¹, M. Ouchrif^{135d}, F. Ould-Saada¹¹⁹, A. Ouraou¹³⁶, K.P. Oussoren¹⁰⁷, Q. Ouyang^{34a}, M. Owen⁵⁴, R.E. Owen¹⁸, V.E. Ozcan^{19a}, N. Ozturk⁸, K. Pachal¹⁴², A. Pacheco Pages¹², C. Padilla Aranda¹², M. Pagáčová⁴⁹, S. Pagan Griso¹⁵, F. Paige²⁶, P. Pais⁸⁷, K. Pajchel¹¹⁹, G. Palacino^{159b}, S. Palestini³¹, M. Palka^{39b}, D. Pallin³⁵, A. Palma^{126a,126b}, E.St. Panagiotopoulou¹⁰, C.E. Pandini⁸¹, J.G. Panduro Vazquez⁷⁸, P. Pani^{146a,146b}, S. Panitkin²⁶, D. Pantea^{27b}, L. Paolozzi⁵⁰, Th.D. Papadopoulos¹⁰, K. Papageorgiou¹⁵⁴, A. Paramonov⁶, D. Paredes Hernandez¹⁷⁵, A.J. Parker⁷³, M.A. Parker²⁹, K.A. Parker¹³⁹, F. Parodi^{51a,51b}, J.A. Parsons³⁶, U. Parzefall⁴⁹, V. Pascuzzi¹⁵⁸, E. Pasqualucci^{132a}, S. Passaggio^{51a}, F. Pastore^{134a,134b,*}, Fr. Pastore⁷⁸, G. Pásztor³⁰, S. Patariaia¹⁷⁴, N.D. Patel¹⁵⁰, J.R. Pater⁸⁵, T. Pauly³¹, J. Pearce¹⁶⁸, B. Pearson¹¹³, L.E. Pedersen³⁷, M. Pedersen¹¹⁹, S. Pedraza Lopez¹⁶⁶, R. Pedro^{126a,126b}, S.V. Peleganchuk^{109,c}, D. Pelikan¹⁶⁴, O. Penc¹²⁷, C. Peng^{34a}, H. Peng^{34b}, J. Penwell⁶², B.S. Peralva^{25b}, M.M. Perego¹³⁶, D.V. Perepelitsa²⁶, E. Perez Codina^{159a}, L. Perini^{92a,92b}, H. Pernegger³¹, S. Perrella^{104a,104b}, R. Peschke⁴³, V.D. Peshekhonov⁶⁶, K. Peters³¹, R.F.Y. Peters⁸⁵, B.A. Petersen³¹, T.C. Petersen³⁷, E. Petit⁵⁶, A. Petridis¹, C. Petridou¹⁵⁴, P. Petroff¹¹⁷, E. Petrolo^{132a}, M. Petrov¹²⁰, F. Petrucci^{134a,134b}, N.E. Pettersson¹⁵⁷, A. Peyaud¹³⁶, R. Pezoa^{33b}, P.W. Phillips¹³¹, G. Piacquadio¹⁴³, E. Pianori¹⁶⁹, A. Picazio⁸⁷, E. Piccaro⁷⁷, M. Piccinini^{21a,21b}, M.A. Pickering¹²⁰, R. Piegaia²⁸, J.E. Pilcher³², A.D. Pilkington⁸⁵, A.W.J. Pin⁸⁵, J. Pina^{126a,126b,126d}, M. Pinamonti^{163a,163c,ae}, J.L. Pinfold³, A. Pingel³⁷, S. Pires⁸¹, H. Pirumov⁴³, M. Pitt¹⁷¹, L. Plazak^{144a}, M.-A. Pleier²⁶, V. Pleskot⁸⁴, E. Plotnikova⁶⁶, P. Plucinski^{146a,146b}, D. Pluth⁶⁵, R. Poettgen^{146a,146b}, L. Poggioli¹¹⁷, D. Pohl²², G. Polesello^{121a}, A. Poley⁴³, A. Policicchio^{38a,38b}, R. Polifka¹⁵⁸, A. Polini^{21a}, C.S. Pollard⁵⁴, V. Polychronakos²⁶, K. Pommès³¹, L. Pontecorvo^{132a}, B.G. Pope⁹¹, G.A. Popeneciu^{27c}, D.S. Popovic¹³, A. Poppleton³¹, S. Pospisil¹²⁸, K. Potamianos¹⁵, I.N. Potrap⁶⁶, C.J. Potter²⁹, C.T. Potter¹¹⁶, G. Poulard³¹, J. Poveda³¹, V. Pozdnyakov⁶⁶, M.E. Pozo Astigarraga³¹, P. Pralavorio⁸⁶, A. Pranko¹⁵, S. Prell⁶⁵, D. Price⁸⁵, L.E. Price⁶, M. Primavera^{74a}, S. Prince⁸⁸, M. Proissl⁴⁷, K. Prokofiev^{61c}, F. Prokoshin^{33b}, S. Protopopescu²⁶, J. Proudfoot⁶, M. Przybycien^{39a}, D. Puddu^{134a,134b}, D. Puldon¹⁴⁸, M. Purohit^{26,af}, P. Puzo¹¹⁷, J. Qian⁹⁰, G. Qin⁵⁴, Y. Qin⁸⁵, A. Quadt⁵⁵, W.B. Quayle^{163a,163b}, M. Queitsch-Maitland⁸⁵, D. Quilty⁵⁴, S. Raddum¹¹⁹, V. Radeka²⁶, V. Radescu^{59b}, S.K. Radhakrishnan¹⁴⁸, P. Radloff¹¹⁶, P. Rados⁸⁹, F. Ragusa^{92a,92b}, G. Rahal¹⁷⁷, J.A. Raine⁸⁵, S. Rajagopalan²⁶, M. Rammensee³¹, C. Rangel-Smith¹⁶⁴, M.G. Ratti^{92a,92b}, F. Rauscher¹⁰⁰, S. Rave⁸⁴, T. Ravenscroft⁵⁴, M. Raymond³¹, A.L. Read¹¹⁹, N.P. Readioff⁷⁵, D.M. Rebuzzi^{121a,121b}, A. Redelbach¹⁷³, G. Redlinger²⁶, R. Reece¹³⁷, K. Reeves⁴², L. Rehnisch¹⁶, J. Reichert¹²², H. Reisin²⁸, C. Rembser³¹, H. Ren^{34a}, M. Rescigno^{132a}, S. Resconi^{92a}, O.L. Rezanova^{109,c}, P. Reznicek¹²⁹, R. Rezvani⁹⁵, R. Richter¹⁰¹, S. Richter⁷⁹, E. Richter-Was^{39b}, O. Ricken²², M. Ridel⁸¹, P. Rieck¹⁶, C.J. Riegel¹⁷⁴, J. Rieger⁵⁵, O. Rifki¹¹³, M. Rijssenbeek¹⁴⁸, A. Rimoldi^{121a,121b}, L. Rinaldi^{21a}, B. Ristić⁵⁰, E. Ritsch³¹, I. Riu¹², F. Rizatdinova¹¹⁴, E. Rizvi⁷⁷, C. Rizzi¹², S.H. Robertson^{88,l}, A. Robichaud-Veronneau⁸⁸, D. Robinson²⁹, J.E.M. Robinson⁴³, A. Robson⁵⁴, C. Roda^{124a,124b}, Y. Rodina⁸⁶, A. Rodriguez Perez¹², D. Rodriguez Rodriguez¹⁶⁶, S. Roe³¹, C.S. Rogan⁵⁸, O. Røhne¹¹⁹, A. Romaniouk⁹⁸, M. Romano^{21a,21b}, S.M. Romano Saez³⁵, E. Romero Adam¹⁶⁶, N. Rompotis¹³⁸, M. Ronzani⁴⁹, L. Roos⁸¹, E. Ros¹⁶⁶, S. Rosati^{132a}, K. Rosbach⁴⁹, P. Rose¹³⁷, O. Rosenthal¹⁴¹, V. Rossetti^{146a,146b}, E. Rossi^{104a,104b}, L.P. Rossi^{51a}, J.H.N. Rosten²⁹, R. Rosten¹³⁸, M. Rotaru^{27b}, I. Roth¹⁷¹, J. Rothberg¹³⁸, D. Rousseau¹¹⁷, C.R. Royon¹³⁶, A. Rozanov⁸⁶, Y. Rozen¹⁵², X. Ruan^{145c}, F. Rubbo¹⁴³, I. Rubinskiy⁴³, V.I. Rud⁹⁹, M.S. Rudolph¹⁵⁸, F. Rühr⁴⁹, A. Ruiz-Martinez³¹, Z. Rurikova⁴⁹, N.A. Rusakovich⁶⁶, A. Ruschke¹⁰⁰, H.L. Russell¹³⁸, J.P. Rutherford⁷, N. Ruthmann³¹, Y.F. Ryabov¹²³, M. Rybar¹⁶⁵, G. Rybkin¹¹⁷, S. Ryu⁶, A. Ryzhov¹³⁰, A.F. Saavedra¹⁵⁰, G. Sabato¹⁰⁷, S. Sacerdoti²⁸, H.F.-W. Sadrozinski¹³⁷, R. Sadykov⁶⁶, F. Safai Tehrani^{132a}, P. Saha¹⁰⁸,

M. Sahinsoy^{59a}, M. Saimpert¹³⁶, T. Saito¹⁵⁵, H. Sakamoto¹⁵⁵, Y. Sakurai¹⁷⁰, G. Salamanna^{134a,134b}, A. Salamon^{133a,133b}, J.E. Salazar Loyola^{33b}, D. Salek¹⁰⁷, P.H. Sales De Bruin¹³⁸, D. Salihagic¹⁰¹, A. Salnikov¹⁴³, J. Salt¹⁶⁶, D. Salvatore^{38a,38b}, F. Salvatore¹⁴⁹, A. Salvucci^{61a}, A. Salzburger³¹, D. Sammel⁴⁹, D. Sampsonidis¹⁵⁴, A. Sanchez^{104a,104b}, J. Sánchez¹⁶⁶, V. Sanchez Martinez¹⁶⁶, H. Sandaker¹¹⁹, R.L. Sandbach⁷⁷, H.G. Sander⁸⁴, M.P. Sanders¹⁰⁰, M. Sandhoff¹⁷⁴, C. Sandoval²⁰, R. Sandstroem¹⁰¹, D.P.C. Sankey¹³¹, M. Sannino^{51a,51b}, A. Sansoni⁴⁸, C. Santoni³⁵, R. Santonico^{133a,133b}, H. Santos^{126a}, I. Santoyo Castillo¹⁴⁹, K. Sapp¹²⁵, A. Sapronov⁶⁶, J.G. Saraiva^{126a,126d}, B. Sarrazin²², O. Sasaki⁶⁷, Y. Sasaki¹⁵⁵, K. Sato¹⁶⁰, G. Sauvage^{5,*}, E. Sauvan⁵, G. Savage⁷⁸, P. Savard^{158,d}, C. Sawyer¹³¹, L. Sawyer^{80,o}, J. Saxon³², C. Sbarra^{21a}, A. Sbrizzi^{21a,21b}, T. Scanlon⁷⁹, D.A. Scannicchio¹⁶², M. Scarcella¹⁵⁰, V. Scarfone^{38a,38b}, J. Schaarschmidt¹⁷¹, P. Schacht¹⁰¹, D. Schaefer³¹, R. Schaefer⁴³, J. Schaeffer⁸⁴, S. Schaepe²², S. Schaetzel^{59b}, U. Schäfer⁸⁴, A.C. Schaffer¹¹⁷, D. Schaile¹⁰⁰, R.D. Schamberger¹⁴⁸, V. Scharf^{59a}, V.A. Schegelsky¹²³, D. Scheirich¹²⁹, M. Schernau¹⁶², C. Schiavi^{51a,51b}, C. Schillo⁴⁹, M. Schioppa^{38a,38b}, S. Schlenker³¹, K. Schmieden³¹, C. Schmitt⁸⁴, S. Schmitt⁴³, S. Schmitz⁸⁴, B. Schneider^{159a}, Y.J. Schnellbach⁷⁵, U. Schnoor⁴⁹, L. Schoeffel¹³⁶, A. Schoening^{59b}, B.D. Schoenrock⁹¹, E. Schopf²², A.L.S. Schorlemmer⁴⁴, M. Schott⁸⁴, J. Schovancova⁸, S. Schramm⁵⁰, M. Schreyer¹⁷³, N. Schuh⁸⁴, M.J. Schultens²², H.-C. Schultz-Coulon^{59a}, H. Schulz¹⁶, M. Schumacher⁴⁹, B.A. Schumm¹³⁷, Ph. Schune¹³⁶, C. Schwanenberger⁸⁵, A. Schwartzman¹⁴³, T.A. Schwarz⁹⁰, Ph. Schwegler¹⁰¹, H. Schweiger⁸⁵, Ph. Schwemling¹³⁶, R. Schwienhorst⁹¹, J. Schwindling¹³⁶, T. Schwindt²², G. Sciolla²⁴, F. Scuri^{124a,124b}, F. Scutti⁸⁹, J. Searcy⁹⁰, P. Seema²², S.C. Seidel¹⁰⁵, A. Seiden¹³⁷, F. Seifert¹²⁸, J.M. Seixas^{25a}, G. Sekhniaidze^{104a}, K. Sekhon⁹⁰, S.J. Sekula⁴¹, D.M. Seliverstov^{123,*}, N. Semprini-Cesari^{21a,21b}, C. Serfon¹¹⁹, L. Serin¹¹⁷, L. Serkin^{163a,163b}, M. Sessa^{134a,134b}, R. Seuster^{159a}, H. Severini¹¹³, T. Sfiligoj⁷⁶, F. Sforza³¹, A. Sfyrla⁵⁰, E. Shabalina⁵⁵, N.W. Shaikh^{146a,146b}, L.Y. Shan^{34a}, R. Shang¹⁶⁵, J.T. Shank²³, M. Shapiro¹⁵, P.B. Shatalov⁹⁷, K. Shaw^{163a,163b}, S.M. Shaw⁸⁵, A. Shcherbakova^{146a,146b}, C.Y. Shehu¹⁴⁹, P. Sherwood⁷⁹, L. Shi^{151,ag}, S. Shimizu⁶⁸, C.O. Shimmin¹⁶², M. Shimojima¹⁰², M. Shiyakova^{66,ah}, A. Shmeleva⁹⁶, D. Shoaleh Saadi⁹⁵, M.J. Shochet³², S. Shojaii^{92a,92b}, S. Shrestha¹¹¹, E. Shulga⁹⁸, M.A. Shupe⁷, P. Sicho¹²⁷, P.E. Sidebo¹⁴⁷, O. Sidiropoulou¹⁷³, D. Sidorov¹¹⁴, A. Sidoti^{21a,21b}, F. Siegert⁴⁵, Dj. Sijacki¹³, J. Silva^{126a,126d}, S.B. Silverstein^{146a}, V. Simak¹²⁸, O. Simard⁵, Lj. Simic¹³, S. Simion¹¹⁷, E. Simioni⁸⁴, B. Simmons⁷⁹, D. Simon³⁵, M. Simon⁸⁴, P. Sinervo¹⁵⁸, N.B. Sinev¹¹⁶, M. Sioli^{21a,21b}, G. Siragusa¹⁷³, S.Yu. Sivoklokov⁹⁹, J. Sjölín^{146a,146b}, T.B. Sjsursen¹⁴, M.B. Skinner⁷³, H.P. Skottowe⁵⁸, P. Skubic¹¹³, M. Slater¹⁸, T. Slavicek¹²⁸, M. Slawinska¹⁰⁷, K. Sliwa¹⁶¹, R. Slovak¹²⁹, V. Smakhtin¹⁷¹, B.H. Smart⁵, L. Smestad¹⁴, S.Yu. Smirnov⁹⁸, Y. Smirnov⁹⁸, L.N. Smirnova^{99,ai}, O. Smirnova⁸², M.N.K. Smith³⁶, R.W. Smith³⁶, M. Smizanska⁷³, K. Smolek¹²⁸, A.A. Snesarev⁹⁶, G. Snidero⁷⁷, S. Snyder²⁶, R. Sobie^{168,l}, F. Socher⁴⁵, A. Soffer¹⁵³, D.A. Soh^{151,ag}, G. Sokhrannyi⁷⁶, C.A. Solans Sanchez³¹, M. Solar¹²⁸, E.Yu. Soldatov⁹⁸, U. Soldevila¹⁶⁶, A.A. Solodkov¹³⁰, A. Soloshenko⁶⁶, O.V. Solovyanov¹³⁰, V. Solovyev¹²³, P. Sommer⁴⁹, H. Son¹⁶¹, H.Y. Song^{34b,z}, A. Sood¹⁵, A. Sopczak¹²⁸, V. Sopko¹²⁸, V. Sorin¹², D. Sosa^{59b}, C.L. Sotiropoulou^{124a,124b}, R. Soualah^{163a,163c}, A.M. Soukharev^{109,c}, D. South⁴³, B.C. Sowden⁷⁸, S. Spagnolo^{74a,74b}, M. Spalla^{124a,124b}, M. Spangenberg¹⁶⁹, F. Spanò⁷⁸, D. Sperlich¹⁶, F. Spettel¹⁰¹, R. Spighi^{21a}, G. Spigo³¹, L.A. Spiller⁸⁹, M. Spousta¹²⁹, R.D. St. Denis^{54,*}, A. Stabile^{92a}, S. Staerz³¹, J. Stahlman¹²², R. Stamen^{59a}, S. Stamm¹⁶, E. Stanecka⁴⁰, R.W. Stanek⁶, C. Stanescu^{134a}, M. Stanescu-Bellu⁴³, M.M. Stanitzki⁴³, S. Stapnes¹¹⁹, E.A. Starchenko¹³⁰, G.H. Stark³², J. Stark⁵⁶, P. Staroba¹²⁷, P. Starovoitov^{59a}, R. Staszewski⁴⁰, P. Steinberg²⁶, B. Stelzer¹⁴², H.J. Stelzer³¹, O. Stelzer-Chilton^{159a}, H. Stenzel⁵³, G.A. Stewart⁵⁴, J.A. Stillings²², M.C. Stockton⁸⁸, M. Stoebe⁸⁸, G. Stoica^{27b}, P. Stolte⁵⁵, S. Stonjek¹⁰¹, A.R. Stradling⁸, A. Straessner⁴⁵, M.E. Stramaglia¹⁷, J. Strandberg¹⁴⁷, S. Strandberg^{146a,146b}, A. Strandlie¹¹⁹, M. Strauss¹¹³, P. Strizenec^{144b}, R. Ströhmer¹⁷³, D.M. Strom¹¹⁶, R. Stroynowski⁴¹, A. Strubig¹⁰⁶, S.A. Stucci¹⁷, B. Stugu¹⁴, N.A. Styles⁴³, D. Su¹⁴³, J. Su¹²⁵, R. Subramaniam⁸⁰, S. Suchek^{59a}, Y. Sugaya¹¹⁸, M. Suk¹²⁸, V.V. Sulín⁹⁶, S. Sultansoy^{4c}, T. Sumida⁶⁹, S. Sun⁵⁸, X. Sun^{34a}, J.E. Sundermann⁴⁹, K. Suruliz¹⁴⁹, G. Susinno^{38a,38b}, M.R. Sutton¹⁴⁹, S. Suzuki⁶⁷, M. Svatos¹²⁷, M. Swiatlowski³², I. Sykora^{144a}, T. Sykora¹²⁹, D. Ta⁴⁹, C. Taccini^{134a,134b}, K. Tackmann⁴³, J. Taenzer¹⁵⁸, A. Taffard¹⁶², R. Tafirout^{159a}, N. Taiblum¹⁵³, H. Takai²⁶, R. Takashima⁷⁰, H. Takeda⁶⁸, T. Takeshita¹⁴⁰, Y. Takubo⁶⁷, M. Talby⁸⁶, A.A. Talyshev^{109,c}, J.Y.C. Tam¹⁷³, K.G. Tan⁸⁹, J. Tanaka¹⁵⁵, R. Tanaka¹¹⁷, S. Tanaka⁶⁷, B.B. Tannenwald¹¹¹, S. Tapia Araya^{33b}, S. Tapprogge⁸⁴,

S. Tarem ¹⁵², G.F. Tartarelli ^{92a}, P. Tas ¹²⁹, M. Tasevsky ¹²⁷, T. Tashiro ⁶⁹, E. Tassi ^{38a,38b},
A. Tavares Delgado ^{126a,126b}, Y. Tayalati ^{135d}, A.C. Taylor ¹⁰⁵, G.N. Taylor ⁸⁹, P.T.E. Taylor ⁸⁹, W. Taylor ^{159b},
F.A. Teischinger ³¹, P. Teixeira-Dias ⁷⁸, K.K. Temming ⁴⁹, D. Temple ¹⁴², H. Ten Kate ³¹, P.K. Teng ¹⁵¹,
J.J. Teoh ¹¹⁸, F. Tepel ¹⁷⁴, S. Terada ⁶⁷, K. Terashi ¹⁵⁵, J. Terron ⁸³, S. Terzo ¹⁰¹, M. Testa ⁴⁸, R.J. Teuscher ^{158,1},
T. Theveneaux-Pelzer ⁸⁶, J.P. Thomas ¹⁸, J. Thomas-Wilsker ⁷⁸, E.N. Thompson ³⁶, P.D. Thompson ¹⁸,
R.J. Thompson ⁸⁵, A.S. Thompson ⁵⁴, L.A. Thomsen ¹⁷⁵, E. Thomson ¹²², M. Thomson ²⁹, M.J. Tibbetts ¹⁵,
R.E. Ticse Torres ⁸⁶, V.O. Tikhomirov ^{96,aj}, Yu.A. Tikhonov ^{109,c}, S. Timoshenko ⁹⁸, P. Tipton ¹⁷⁵,
S. Tisserant ⁸⁶, K. Todome ¹⁵⁷, T. Todorov ^{5,*}, S. Todorova-Nova ¹²⁹, J. Tojo ⁷¹, S. Tokár ^{144a},
K. Tokushuku ⁶⁷, E. Tolley ⁵⁸, L. Tomlinson ⁸⁵, M. Tomoto ¹⁰³, L. Tompkins ^{143,ak}, K. Toms ¹⁰⁵, B. Tong ⁵⁸,
E. Torrence ¹¹⁶, H. Torres ¹⁴², E. Torró Pastor ¹³⁸, J. Toth ^{86,al}, F. Touchard ⁸⁶, D.R. Tovey ¹³⁹, T. Trefzger ¹⁷³,
L. Tremblet ³¹, A. Tricoli ³¹, I.M. Trigger ^{159a}, S. Trincaz-Duvoid ⁸¹, M.F. Tripiana ¹², W. Trischuk ¹⁵⁸,
B. Trocmé ⁵⁶, A. Trofymov ⁴³, C. Troncon ^{92a}, M. Trottier-McDonald ¹⁵, M. Trovatelli ¹⁶⁸, L. Truong ^{163a,163b},
M. Trzebinski ⁴⁰, A. Trzupek ⁴⁰, J.C.-L. Tseng ¹²⁰, P.V. Tsiarehsha ⁹³, G. Tsipolitis ¹⁰, N. Tsirintanis ⁹,
S. Tsiskaridze ¹², V. Tsiskaridze ⁴⁹, E.G. Tskhadadze ^{52a}, K.M. Tsui ^{61a}, I.I. Tsukerman ⁹⁷, V. Tsulaia ¹⁵,
S. Tsuno ⁶⁷, D. Tsybychev ¹⁴⁸, A. Tudorache ^{27b}, V. Tudorache ^{27b}, A.N. Tuna ⁵⁸, S.A. Tupputi ^{21a,21b},
S. Turchikhin ^{99,ai}, D. Turecek ¹²⁸, D. Turgeman ¹⁷¹, R. Turra ^{92a,92b}, A.J. Turvey ⁴¹, P.M. Tuts ³⁶,
M. Tyndel ¹³¹, G. Ucchielli ^{21a,21b}, I. Ueda ¹⁵⁵, R. Ueno ³⁰, M. Ughetto ^{146a,146b}, F. Ukegawa ¹⁶⁰, G. Unal ³¹,
A. Undrus ²⁶, G. Unel ¹⁶², F.C. Ungaro ⁸⁹, Y. Unno ⁶⁷, C. Unverdorben ¹⁰⁰, J. Urban ^{144b}, P. Urquijo ⁸⁹,
P. Urrejola ⁸⁴, G. Usai ⁸, A. Usanova ⁶³, L. Vacavant ⁸⁶, V. Vacek ¹²⁸, B. Vachon ⁸⁸, C. Valderanis ¹⁰⁰,
E. Valdes Santurio ^{146a,146b}, N. Valencic ¹⁰⁷, S. Valentini ^{21a,21b}, A. Valero ¹⁶⁶, L. Valery ¹², S. Valkar ¹²⁹,
S. Vallecorsa ⁵⁰, J.A. Valls Ferrer ¹⁶⁶, W. Van Den Wollenberg ¹⁰⁷, P.C. Van Der Deijl ¹⁰⁷,
R. van der Geer ¹⁰⁷, H. van der Graaf ¹⁰⁷, N. van Eldik ¹⁵², P. van Gemmeren ⁶, J. Van Nieuwkoop ¹⁴²,
I. van Vulpen ¹⁰⁷, M.C. van Woerden ³¹, M. Vanadia ^{132a,132b}, W. Vandelli ³¹, R. Vanguri ¹²²,
A. Vaniachine ⁶, P. Vankov ¹⁰⁷, G. Vardanyan ¹⁷⁶, R. Vari ^{132a}, E.W. Varnes ⁷, T. Varol ⁴¹, D. Varouchas ⁸¹,
A. Vartapetian ⁸, K.E. Varvell ¹⁵⁰, J.G. Vasquez ¹⁷⁵, F. Vazeille ³⁵, T. Vazquez Schroeder ⁸⁸, J. Veatch ⁵⁵,
L.M. Veloce ¹⁵⁸, F. Veloso ^{126a,126c}, S. Veneziano ^{132a}, A. Ventura ^{74a,74b}, M. Venturi ¹⁶⁸, N. Venturi ¹⁵⁸,
A. Venturini ²⁴, V. Vercesi ^{121a}, M. Verducci ^{132a,132b}, W. Verkerke ¹⁰⁷, J.C. Vermeulen ¹⁰⁷, A. Vest ^{45,am},
M.C. Vetterli ^{142,d}, O. Viazlo ⁸², I. Vichou ¹⁶⁵, T. Vickey ¹³⁹, O.E. Vickey Boeriu ¹³⁹, G.H.A. Viehhauser ¹²⁰,
S. Viel ¹⁵, L. Vigani ¹²⁰, R. Vigne ⁶³, M. Villa ^{21a,21b}, M. Villaplana Perez ^{92a,92b}, E. Vilucchi ⁴⁸,
M.G. Vincker ³⁰, V.B. Vinogradov ⁶⁶, C. Vittori ^{21a,21b}, I. Vivarelli ¹⁴⁹, S. Vlachos ¹⁰, M. Vlasak ¹²⁸,
M. Vogel ¹⁷⁴, P. Vokac ¹²⁸, G. Volpi ^{124a,124b}, M. Volpi ⁸⁹, H. von der Schmitt ¹⁰¹, E. von Toerne ²²,
V. Vorobel ¹²⁹, K. Vorobev ⁹⁸, M. Vos ¹⁶⁶, R. Voss ³¹, J.H. Vossebeld ⁷⁵, N. Vranjes ¹³,
M. Vranjes Milosavljevic ¹³, V. Vrba ¹²⁷, M. Vreeswijk ¹⁰⁷, R. Vuillermet ³¹, I. Vukotic ³², Z. Vykydal ¹²⁸,
P. Wagner ²², W. Wagner ¹⁷⁴, H. Wahlberg ⁷², S. Wahrmund ⁴⁵, J. Wakabayashi ¹⁰³, J. Walder ⁷³,
R. Walker ¹⁰⁰, W. Walkowiak ¹⁴¹, V. Wallangen ^{146a,146b}, C. Wang ¹⁵¹, C. Wang ^{34d,86}, F. Wang ¹⁷²,
H. Wang ¹⁵, H. Wang ⁴¹, J. Wang ⁴³, J. Wang ¹⁵⁰, K. Wang ⁸⁸, R. Wang ⁶, S.M. Wang ¹⁵¹, T. Wang ²²,
T. Wang ³⁶, X. Wang ¹⁷⁵, C. Wanotayaroj ¹¹⁶, A. Warburton ⁸⁸, C.P. Ward ²⁹, D.R. Wardrope ⁷⁹,
A. Washbrook ⁴⁷, P.M. Watkins ¹⁸, A.T. Watson ¹⁸, I.J. Watson ¹⁵⁰, M.F. Watson ¹⁸, G. Watts ¹³⁸, S. Watts ⁸⁵,
B.M. Waugh ⁷⁹, S. Webb ⁸⁴, M.S. Weber ¹⁷, S.W. Weber ¹⁷³, J.S. Webster ⁶, A.R. Weidberg ¹²⁰, B. Weinert ⁶²,
J. Weingarten ⁵⁵, C. Weiser ⁴⁹, H. Weits ¹⁰⁷, P.S. Wells ³¹, T. Wenaus ²⁶, T. Wengler ³¹, S. Wenig ³¹,
N. Vermes ²², M. Werner ⁴⁹, P. Werner ³¹, M. Wessels ^{59a}, J. Wetter ¹⁶¹, K. Whalen ¹¹⁶, N.L. Whallon ¹³⁸,
A.M. Wharton ⁷³, A. White ⁸, M.J. White ¹, R. White ^{33b}, S. White ^{124a,124b}, D. Whiteson ¹⁶²,
F.J. Wickens ¹³¹, W. Wiedenmann ¹⁷², M. Wielers ¹³¹, P. Wienemann ²², C. Wigglesworth ³⁷,
L.A.M. Wiik-Fuchs ²², A. Wildauer ¹⁰¹, F. Wilk ⁸⁵, H.G. Wilkens ³¹, H.H. Williams ¹²², S. Williams ¹⁰⁷,
C. Willis ⁹¹, S. Willocq ⁸⁷, J.A. Wilson ¹⁸, I. Wingerter-Seetz ⁵, F. Winklmeier ¹¹⁶, O.J. Winston ¹⁴⁹,
B.T. Winter ²², M. Wittgen ¹⁴³, J. Wittkowski ¹⁰⁰, S.J. Wollstadt ⁸⁴, M.W. Wolter ⁴⁰, H. Wolters ^{126a,126c},
B.K. Wosiek ⁴⁰, J. Wotschack ³¹, M.J. Woudstra ⁸⁵, K.W. Wozniak ⁴⁰, M. Wu ⁵⁶, M. Wu ³², S.L. Wu ¹⁷²,
X. Wu ⁵⁰, Y. Wu ⁹⁰, T.R. Wyatt ⁸⁵, B.M. Wynne ⁴⁷, S. Xella ³⁷, D. Xu ^{34a}, L. Xu ²⁶, B. Yabsley ¹⁵⁰,
S. Yacoob ^{145a}, R. Yakabe ⁶⁸, D. Yamaguchi ¹⁵⁷, Y. Yamaguchi ¹¹⁸, A. Yamamoto ⁶⁷, S. Yamamoto ¹⁵⁵,
T. Yamanaka ¹⁵⁵, K. Yamauchi ¹⁰³, Y. Yamazaki ⁶⁸, Z. Yan ²³, H. Yang ^{34e}, H. Yang ¹⁷², Y. Yang ¹⁵¹, Z. Yang ¹⁴,
W.-M. Yao ¹⁵, Y.C. Yap ⁸¹, Y. Yasu ⁶⁷, E. Yatsenko ⁵, K.H. Yau Wong ²², J. Ye ⁴¹, S. Ye ²⁶, I. Yeletsikh ⁶⁶,
A.L. Yen ⁵⁸, E. Yildirim ⁴³, K. Yorita ¹⁷⁰, R. Yoshida ⁶, K. Yoshihara ¹²², C. Young ¹⁴³, C.J.S. Young ³¹,

S. Youssef²³, D.R. Yu¹⁵, J. Yu⁸, J.M. Yu⁹⁰, J. Yu⁶⁵, L. Yuan⁶⁸, S.P.Y. Yuen²², I. Yusuff^{29,an}, B. Zabinski⁴⁰, R. Zaidan^{34d}, A.M. Zaitsev^{130,ac}, N. Zakharchuk⁴³, J. Zalieckas¹⁴, A. Zaman¹⁴⁸, S. Zambito⁵⁸, L. Zanello^{132a,132b}, D. Zanzi⁸⁹, C. Zeitnitz¹⁷⁴, M. Zeman¹²⁸, A. Zemla^{39a}, J.C. Zeng¹⁶⁵, Q. Zeng¹⁴³, K. Zengel²⁴, O. Zenin¹³⁰, T. Ženiš^{144a}, D. Zerwas¹¹⁷, D. Zhang⁹⁰, F. Zhang¹⁷², G. Zhang^{34b,z}, H. Zhang^{34c}, J. Zhang⁶, L. Zhang⁴⁹, R. Zhang²², R. Zhang^{34b,ao}, X. Zhang^{34d}, Z. Zhang¹¹⁷, X. Zhao⁴¹, Y. Zhao^{34d,117}, Z. Zhao^{34b}, A. Zhemchugov⁶⁶, J. Zhong¹²⁰, B. Zhou⁹⁰, C. Zhou⁴⁶, L. Zhou³⁶, L. Zhou⁴¹, M. Zhou¹⁴⁸, N. Zhou^{34f}, C.G. Zhu^{34d}, H. Zhu^{34a}, J. Zhu⁹⁰, Y. Zhu^{34b}, X. Zhuang^{34a}, K. Zhukov⁹⁶, A. Zibell¹⁷³, D. Zieminska⁶², N.I. Zimine⁶⁶, C. Zimmermann⁸⁴, S. Zimmermann⁴⁹, Z. Zinonos⁵⁵, M. Zinser⁸⁴, M. Ziolkowski¹⁴¹, L. Živković¹³, G. Zobernig¹⁷², A. Zoccoli^{21a,21b}, M. zur Nedden¹⁶, G. Zurzolo^{104a,104b}, L. Zwalinski³¹

¹ Department of Physics, University of Adelaide, Adelaide, Australia

² Physics Department, SUNY Albany, Albany NY, United States

³ Department of Physics, University of Alberta, Edmonton, AB, Canada

⁴ (a) Department of Physics, Ankara University, Ankara; (b) Istanbul Aydin University, Istanbul; (c) Division of Physics, TOBB University of Economics and Technology, Ankara, Turkey

⁵ LAPP, CNRS/IN2P3 and Université Savoie Mont Blanc, Annecy-le-Vieux, France

⁶ High Energy Physics Division, Argonne National Laboratory, Argonne, IL, United States

⁷ Department of Physics, University of Arizona, Tucson, AZ, United States

⁸ Department of Physics, The University of Texas at Arlington, Arlington, TX, United States

⁹ Physics Department, University of Athens, Athens, Greece

¹⁰ Physics Department, National Technical University of Athens, Zografou, Greece

¹¹ Institute of Physics, Azerbaijan Academy of Sciences, Baku, Azerbaijan

¹² Institut de Física d'Altes Energies (IFAE), The Barcelona Institute of Science and Technology, Barcelona, Spain

¹³ Institute of Physics, University of Belgrade, Belgrade, Serbia

¹⁴ Department for Physics and Technology, University of Bergen, Bergen, Norway

¹⁵ Physics Division, Lawrence Berkeley National Laboratory and University of California, Berkeley CA, United States

¹⁶ Department of Physics, Humboldt University, Berlin, Germany

¹⁷ Albert Einstein Center for Fundamental Physics and Laboratory for High Energy Physics, University of Bern, Bern, Switzerland

¹⁸ School of Physics and Astronomy, University of Birmingham, Birmingham, United Kingdom

¹⁹ (a) Department of Physics, Bogazici University, Istanbul; (b) Department of Physics Engineering, Gaziantep University, Gaziantep; (d) Istanbul Bilgi University, Faculty of Engineering and Natural Sciences, Istanbul, Turkey; (e) Bahcesehir University, Faculty of Engineering and Natural Sciences, Istanbul, Turkey

²⁰ Centro de Investigaciones, Universidad Antonio Narino, Bogota, Colombia

²¹ (a) INFN Sezione di Bologna; (b) Dipartimento di Fisica e Astronomia, Università di Bologna, Bologna, Italy

²² Physikalisches Institut, University of Bonn, Bonn, Germany

²³ Department of Physics, Boston University, Boston, MA, United States

²⁴ Department of Physics, Brandeis University, Waltham, MA, United States

²⁵ (a) Universidade Federal do Rio De Janeiro COPPE/EE/IF, Rio de Janeiro; (b) Electrical Circuits Department, Federal University of Juiz de Fora (UFJF), Juiz de Fora; (c) Federal University of Sao Joao del Rei (UFSJ), Sao Joao del Rei; (d) Instituto de Fisica, Universidade de Sao Paulo, Sao Paulo, Brazil

²⁶ Physics Department, Brookhaven National Laboratory, Upton, NY, United States

²⁷ (a) Transilvania University of Brasov, Brasov, Romania; (b) National Institute of Physics and Nuclear Engineering, Bucharest; (c) National Institute for Research and Development of Isotopic and Molecular Technologies, Physics Department, Cluj Napoca; (d) University Politehnica Bucharest, Bucharest; (e) West University in Timisoara, Timisoara, Romania

²⁸ Departamento de Fisica, Universidad de Buenos Aires, Buenos Aires, Argentina

²⁹ Cavendish Laboratory, University of Cambridge, Cambridge, United Kingdom

³⁰ Department of Physics, Carleton University, Ottawa, ON, Canada

³¹ CERN, Geneva, Switzerland

³² Enrico Fermi Institute, University of Chicago, Chicago, IL, United States

³³ (a) Departamento de Fisica, Pontificia Universidad Católica de Chile, Santiago; (b) Departamento de Fisica, Universidad Técnica Federico Santa María, Valparaíso, Chile

³⁴ (a) Institute of High Energy Physics, Chinese Academy of Sciences, Beijing; (b) Department of Modern Physics, University of Science and Technology of China, Anhui; (c) Department of Physics, Nanjing University, Jiangsu; (d) School of Physics, Shandong University, Shandong; (e) Department of Physics and Astronomy, Shanghai Key Laboratory for Particle Physics and Cosmology, Shanghai Jiao Tong University, Shanghai; (f) Physics Department, Tsinghua University, Beijing 100084, China

³⁵ Laboratoire de Physique Corpusculaire, Clermont Université and Université Blaise Pascal and CNRS/IN2P3, Clermont-Ferrand, France

³⁶ Nevis Laboratory, Columbia University, Irvington, NY, United States

³⁷ Niels Bohr Institute, University of Copenhagen, Copenhagen, Denmark

³⁸ (a) INFN Gruppo Collegato di Cosenza, Laboratori Nazionali di Frascati; (b) Dipartimento di Fisica, Università della Calabria, Rende, Italy

³⁹ (a) AGH University of Science and Technology, Faculty of Physics and Applied Computer Science, Krakow; (b) Marian Smoluchowski Institute of Physics, Jagiellonian University, Krakow, Poland

⁴⁰ Institute of Nuclear Physics Polish Academy of Sciences, Krakow, Poland

⁴¹ Physics Department, Southern Methodist University, Dallas, TX, United States

⁴² Physics Department, University of Texas at Dallas, Richardson, TX, United States

⁴³ DESY, Hamburg and Zeuthen, Germany

⁴⁴ Institut für Experimentelle Physik IV, Technische Universität Dortmund, Dortmund, Germany

⁴⁵ Institut für Kern- und Teilchenphysik, Technische Universität Dresden, Dresden, Germany

⁴⁶ Department of Physics, Duke University, Durham, NC, United States

⁴⁷ SUPA – School of Physics and Astronomy, University of Edinburgh, Edinburgh, United Kingdom

⁴⁸ INFN Laboratori Nazionali di Frascati, Frascati, Italy

⁴⁹ Fakultät für Mathematik und Physik, Albert-Ludwigs-Universität, Freiburg, Germany

⁵⁰ Section de Physique, Université de Genève, Geneva, Switzerland

⁵¹ (a) INFN Sezione di Genova; (b) Dipartimento di Fisica, Università di Genova, Genova, Italy

⁵² (a) E. Andronikashvili Institute of Physics, Iv. Javakishvili Tbilisi State University, Tbilisi; (b) High Energy Physics Institute, Tbilisi State University, Tbilisi, Georgia

⁵³ II Physikalisches Institut, Justus-Liebig-Universität Giessen, Giessen, Germany

⁵⁴ SUPA – School of Physics and Astronomy, University of Glasgow, Glasgow, United Kingdom

⁵⁵ II Physikalisches Institut, Georg-August-Universität, Göttingen, Germany

⁵⁶ Laboratoire de Physique Subatomique et de Cosmologie, Université Grenoble-Alpes, CNRS/IN2P3, Grenoble, France

⁵⁷ Department of Physics, Hampton University, Hampton, VA, United States

- ⁵⁸ Laboratory for Particle Physics and Cosmology, Harvard University, Cambridge, MA, United States
- ⁵⁹ ^(a) Kirchhoff-Institut für Physik, Ruprecht-Karls-Universität Heidelberg, Heidelberg; ^(b) Physikalisches Institut, Ruprecht-Karls-Universität Heidelberg, Heidelberg; ^(c) ZITI Institut für technische Informatik, Ruprecht-Karls-Universität Heidelberg, Mannheim, Germany
- ⁶⁰ Faculty of Applied Information Science, Hiroshima Institute of Technology, Hiroshima, Japan
- ⁶¹ ^(a) Department of Physics, The Chinese University of Hong Kong, Shatin, N.T., Hong Kong; ^(b) Department of Physics, The University of Hong Kong, Hong Kong; ^(c) Department of Physics, The Hong Kong University of Science and Technology, Clear Water Bay, Kowloon, Hong Kong, China
- ⁶² Department of Physics, Indiana University, Bloomington, IN, United States
- ⁶³ Institut für Astro- und Teilchenphysik, Leopold-Franzens-Universität, Innsbruck, Austria
- ⁶⁴ University of Iowa, Iowa City, IA, United States
- ⁶⁵ Department of Physics and Astronomy, Iowa State University, Ames, IA, United States
- ⁶⁶ Joint Institute for Nuclear Research, JINR Dubna, Dubna, Russia
- ⁶⁷ KEK, High Energy Accelerator Research Organization, Tsukuba, Japan
- ⁶⁸ Graduate School of Science, Kobe University, Kobe, Japan
- ⁶⁹ Faculty of Science, Kyoto University, Kyoto, Japan
- ⁷⁰ Kyoto University of Education, Kyoto, Japan
- ⁷¹ Department of Physics, Kyushu University, Fukuoka, Japan
- ⁷² Instituto de Física La Plata, Universidad Nacional de La Plata and CONICET, La Plata, Argentina
- ⁷³ Physics Department, Lancaster University, Lancaster, United Kingdom
- ⁷⁴ ^(a) INFN Sezione di Lecce; ^(b) Dipartimento di Matematica e Fisica, Università del Salento, Lecce, Italy
- ⁷⁵ Oliver Lodge Laboratory, University of Liverpool, Liverpool, United Kingdom
- ⁷⁶ Department of Physics, Jožef Stefan Institute and University of Ljubljana, Ljubljana, Slovenia
- ⁷⁷ School of Physics and Astronomy, Queen Mary University of London, London, United Kingdom
- ⁷⁸ Department of Physics, Royal Holloway University of London, Surrey, United Kingdom
- ⁷⁹ Department of Physics and Astronomy, University College London, London, United Kingdom
- ⁸⁰ Louisiana Tech University, Ruston LA, United States
- ⁸¹ Laboratoire de Physique Nucléaire et de Hautes Energies, UPMC and Université Paris-Diderot and CNRS/IN2P3, Paris, France
- ⁸² Fysiska institutionen, Lunds universitet, Lund, Sweden
- ⁸³ Departamento de Física Teórica C-15, Universidad Autónoma de Madrid, Madrid, Spain
- ⁸⁴ Institut für Physik, Universität Mainz, Mainz, Germany
- ⁸⁵ School of Physics and Astronomy, University of Manchester, Manchester, United Kingdom
- ⁸⁶ CPPM, Aix-Marseille Université and CNRS/IN2P3, Marseille, France
- ⁸⁷ Department of Physics, University of Massachusetts, Amherst, MA, United States
- ⁸⁸ Department of Physics, McGill University, Montreal, QC, Canada
- ⁸⁹ School of Physics, University of Melbourne, Victoria, Australia
- ⁹⁰ Department of Physics, The University of Michigan, Ann Arbor, MI, United States
- ⁹¹ Department of Physics and Astronomy, Michigan State University, East Lansing, MI, United States
- ⁹² ^(a) INFN Sezione di Milano; ^(b) Dipartimento di Fisica, Università di Milano, Milano, Italy
- ⁹³ B.I. Stepanov Institute of Physics, National Academy of Sciences of Belarus, Minsk, Belarus
- ⁹⁴ National Scientific and Educational Centre for Particle and High Energy Physics, Minsk, Belarus
- ⁹⁵ Group of Particle Physics, University of Montreal, Montreal, QC, Canada
- ⁹⁶ P.N. Lebedev Physical Institute of the Russian Academy of Sciences, Moscow, Russia
- ⁹⁷ Institute for Theoretical and Experimental Physics (ITEP), Moscow, Russia
- ⁹⁸ National Research Nuclear University MEPhI, Moscow, Russia
- ⁹⁹ D.V. Skobeltsyn Institute of Nuclear Physics, M.V. Lomonosov Moscow State University, Moscow, Russia
- ¹⁰⁰ Fakultät für Physik, Ludwig-Maximilians-Universität München, München, Germany
- ¹⁰¹ Max-Planck-Institut für Physik (Werner-Heisenberg-Institut), München, Germany
- ¹⁰² Nagasaki Institute of Applied Science, Nagasaki, Japan
- ¹⁰³ Graduate School of Science and Kobayashi–Maskawa Institute, Nagoya University, Nagoya, Japan
- ¹⁰⁴ ^(a) INFN Sezione di Napoli; ^(b) Dipartimento di Fisica, Università di Napoli, Napoli, Italy
- ¹⁰⁵ Department of Physics and Astronomy, University of New Mexico, Albuquerque, NM, United States
- ¹⁰⁶ Institute for Mathematics, Astrophysics and Particle Physics, Radboud University Nijmegen/Nikhef, Nijmegen, Netherlands
- ¹⁰⁷ Nikhef National Institute for Subatomic Physics and University of Amsterdam, Amsterdam, Netherlands
- ¹⁰⁸ Department of Physics, Northern Illinois University, DeKalb, IL, United States
- ¹⁰⁹ Budker Institute of Nuclear Physics, SB RAS, Novosibirsk, Russia
- ¹¹⁰ Department of Physics, New York University, New York, NY, United States
- ¹¹¹ Ohio State University, Columbus OH, United States
- ¹¹² Faculty of Science, Okayama University, Okayama, Japan
- ¹¹³ Homer L. Dodge Department of Physics and Astronomy, University of Oklahoma, Norman, OK, United States
- ¹¹⁴ Department of Physics, Oklahoma State University, Stillwater, OK, United States
- ¹¹⁵ Palacký University, RCPTM, Olomouc, Czech Republic
- ¹¹⁶ Center for High Energy Physics, University of Oregon, Eugene, OR, United States
- ¹¹⁷ LAL, Univ. Paris-Sud, CNRS/IN2P3, Université Paris-Saclay, Orsay, France
- ¹¹⁸ Graduate School of Science, Osaka University, Osaka, Japan
- ¹¹⁹ Department of Physics, University of Oslo, Oslo, Norway
- ¹²⁰ Department of Physics, Oxford University, Oxford, United Kingdom
- ¹²¹ ^(a) INFN Sezione di Pavia; ^(b) Dipartimento di Fisica, Università di Pavia, Pavia, Italy
- ¹²² Department of Physics, University of Pennsylvania, Philadelphia, PA, United States
- ¹²³ National Research Centre “Kurchatov Institute”, B.P. Konstantinov Petersburg Nuclear Physics Institute, St. Petersburg, Russia
- ¹²⁴ ^(a) INFN Sezione di Pisa; ^(b) Dipartimento di Fisica E. Fermi, Università di Pisa, Pisa, Italy
- ¹²⁵ Department of Physics and Astronomy, University of Pittsburgh, Pittsburgh, PA, United States
- ¹²⁶ ^(a) Laboratório de Instrumentação e Física Experimental de Partículas – LIP, Lisboa; ^(b) Faculdade de Ciências, Universidade de Lisboa, Lisboa; ^(c) Department of Physics, University of Coimbra, Coimbra; ^(d) Centro de Física Nuclear da Universidade de Lisboa, Lisboa; ^(e) Departamento de Física, Universidade do Minho, Braga; ^(f) Departamento de Física Teórica y del Cosmos and CAFPE, Universidad de Granada, Granada (Spain); ^(g) Dep Física and CEFITEC of Faculdade de Ciências e Tecnologia, Universidade Nova de Lisboa, Caparica, Portugal
- ¹²⁷ Institute of Physics, Academy of Sciences of the Czech Republic, Praha, Czech Republic
- ¹²⁸ Czech Technical University in Prague, Praha, Czech Republic
- ¹²⁹ Faculty of Mathematics and Physics, Charles University in Prague, Praha, Czech Republic
- ¹³⁰ State Research Center Institute for High Energy Physics (Protvino), NRC KI, Russia
- ¹³¹ Particle Physics Department, Rutherford Appleton Laboratory, Didcot, United Kingdom
- ¹³² ^(a) INFN Sezione di Roma; ^(b) Dipartimento di Fisica, Sapienza Università di Roma, Roma, Italy

- 133 ^(a) INFN Sezione di Roma Tor Vergata; ^(b) Dipartimento di Fisica, Università di Roma Tor Vergata, Roma, Italy
- 134 ^(a) INFN Sezione di Roma Tre; ^(b) Dipartimento di Matematica e Fisica, Università Roma Tre, Roma, Italy
- 135 ^(a) Faculté des Sciences Ain Chock, Réseau Universitaire de Physique des Hautes Energies – Université Hassan II, Casablanca; ^(b) Centre National de l'Energie des Sciences Techniques Nucleaires, Rabat; ^(c) Faculté des Sciences Semlalia, Université Cadi Ayyad, LPHEA-Marrakech; ^(d) Faculté des Sciences, Université Mohamed Premier and LPTPM, Oujda; ^(e) Faculté des sciences, Université Mohammed V, Rabat, Morocco
- 136 DSM/IRFU (Institut de Recherches sur les Lois Fondamentales de l'Univers), CEA Saclay (Commissariat à l'Energie Atomique et aux Energies Alternatives), Gif-sur-Yvette, France
- 137 Santa Cruz Institute for Particle Physics, University of California Santa Cruz, Santa Cruz CA, United States
- 138 Department of Physics, University of Washington, Seattle, WA, United States
- 139 Department of Physics and Astronomy, University of Sheffield, Sheffield, United Kingdom
- 140 Department of Physics, Shinshu University, Nagano, Japan
- 141 Fachbereich Physik, Universität Siegen, Siegen, Germany
- 142 Department of Physics, Simon Fraser University, Burnaby, BC, Canada
- 143 SLAC National Accelerator Laboratory, Stanford CA, United States
- 144 ^(a) Faculty of Mathematics, Physics & Informatics, Comenius University, Bratislava; ^(b) Department of Subnuclear Physics, Institute of Experimental Physics of the Slovak Academy of Sciences, Kosice, Slovak Republic
- 145 ^(a) Department of Physics, University of Cape Town, Cape Town; ^(b) Department of Physics, University of Johannesburg, Johannesburg; ^(c) School of Physics, University of the Witwatersrand, Johannesburg, South Africa
- 146 ^(a) Department of Physics, Stockholm University; ^(b) The Oskar Klein Centre, Stockholm, Sweden
- 147 Physics Department, Royal Institute of Technology, Stockholm, Sweden
- 148 Departments of Physics & Astronomy and Chemistry, Stony Brook University, Stony Brook NY, United States
- 149 Department of Physics and Astronomy, University of Sussex, Brighton, United Kingdom
- 150 School of Physics, University of Sydney, Sydney, Australia
- 151 Institute of Physics, Academia Sinica, Taipei, Taiwan
- 152 Department of Physics, Technion: Israel Institute of Technology, Haifa, Israel
- 153 Raymond and Beverly Sackler School of Physics and Astronomy, Tel Aviv University, Tel Aviv, Israel
- 154 Department of Physics, Aristotle University of Thessaloniki, Thessaloniki, Greece
- 155 International Center for Elementary Particle Physics and Department of Physics, The University of Tokyo, Tokyo, Japan
- 156 Graduate School of Science and Technology, Tokyo Metropolitan University, Tokyo, Japan
- 157 Department of Physics, Tokyo Institute of Technology, Tokyo, Japan
- 158 Department of Physics, University of Toronto, Toronto, ON, Canada
- 159 ^(a) TRIUMF, Vancouver BC; ^(b) Department of Physics and Astronomy, York University, Toronto, ON, Canada
- 160 Faculty of Pure and Applied Sciences, and Center for Integrated Research in Fundamental Science and Engineering, University of Tsukuba, Tsukuba, Japan
- 161 Department of Physics and Astronomy, Tufts University, Medford, MA, United States
- 162 Department of Physics and Astronomy, University of California Irvine, Irvine, CA, United States
- 163 ^(a) INFN Gruppo Collegato di Udine, Sezione di Trieste, Udine; ^(b) ICTP, Trieste; ^(c) Dipartimento di Chimica, Fisica e Ambiente, Università di Udine, Udine, Italy
- 164 Department of Physics and Astronomy, University of Uppsala, Uppsala, Sweden
- 165 Department of Physics, University of Illinois, Urbana, IL, United States
- 166 Instituto de Física Corpuscular (IFIC) and Departamento de Física Atómica, Molecular y Nuclear and Departamento de Ingeniería Electrónica and Instituto de Microelectrónica de Barcelona (IMB-CNM), University of Valencia and CSIC, Valencia, Spain
- 167 Department of Physics, University of British Columbia, Vancouver, BC, Canada
- 168 Department of Physics and Astronomy, University of Victoria, Victoria, BC, Canada
- 169 Department of Physics, University of Warwick, Coventry, United Kingdom
- 170 Waseda University, Tokyo, Japan
- 171 Department of Particle Physics, The Weizmann Institute of Science, Rehovot, Israel
- 172 Department of Physics, University of Wisconsin, Madison, WI, United States
- 173 Fakultät für Physik und Astronomie, Julius-Maximilians-Universität, Würzburg, Germany
- 174 Fakultät für Mathematik und Naturwissenschaften, Fachgruppe Physik, Bergische Universität Wuppertal, Wuppertal, Germany
- 175 Department of Physics, Yale University, New Haven, CT, United States
- 176 Yerevan Physics Institute, Yerevan, Armenia
- 177 Centre de Calcul de l'Institut National de Physique Nucléaire et de Physique des Particules (IN2P3), Villeurbanne, France

^a Also at Department of Physics, King's College London, London, United Kingdom.

^b Also at Institute of Physics, Azerbaijan Academy of Sciences, Baku, Azerbaijan.

^c Also at Novosibirsk State University, Novosibirsk, Russia.

^d Also at TRIUMF, Vancouver, BC, Canada.

^e Also at Department of Physics & Astronomy, University of Louisville, Louisville, KY, United States.

^f Also at Department of Physics, California State University, Fresno, CA, United States.

^g Also at Department of Physics, University of Fribourg, Fribourg, Switzerland.

^h Also at Departament de Física de la Universitat Autònoma de Barcelona, Barcelona, Spain.

ⁱ Also at Departamento de Física e Astronomia, Faculdade de Ciências, Universidade do Porto, Portugal.

^j Also at Tomsk State University, Tomsk, Russia.

^k Also at Università di Napoli Parthenope, Napoli, Italy.

^l Also at Institute of Particle Physics (IPP), Canada.

^m Also at Department of Physics, St. Petersburg State Polytechnical University, St. Petersburg, Russia.

ⁿ Also at Department of Physics, The University of Michigan, Ann Arbor, MI, United States.

^o Also at Louisiana Tech University, Ruston, LA, United States.

^p Also at Institutio Catalana de Recerca i Estudis Avançats, ICREA, Barcelona, Spain.

^q Also at Graduate School of Science, Osaka University, Osaka, Japan.

^r Also at Department of Physics, National Tsing Hua University, Taiwan.

^s Also at Department of Physics, The University of Texas at Austin, Austin, TX, United States.

^t Also at Institute of Theoretical Physics, Ilia State University, Tbilisi, Georgia.

^u Also at CERN, Geneva, Switzerland.

^v Also at Georgian Technical University (GTU), Tbilisi, Georgia.

^w Also at Ochadai Academic Production, Ochanomizu University, Tokyo, Japan.

^x Also at Manhattan College, New York, NY, United States.

^y Also at Hellenic Open University, Patras, Greece.

^z Also at Institute of Physics, Academia Sinica, Taipei, Taiwan.

^{aa} Also at Academia Sinica Grid Computing, Institute of Physics, Academia Sinica, Taipei, Taiwan.

^{ab} Also at School of Physics, Shandong University, Shandong, China.

^{ac} Also at Moscow Institute of Physics and Technology State University, Dolgoprudny, Russia.

^{ad} Also at Section de Physique, Université de Genève, Geneva, Switzerland.

^{ae} Also at International School for Advanced Studies (SISSA), Trieste, Italy.

^{af} Also at Department of Physics and Astronomy, University of South Carolina, Columbia, SC, United States.

^{ag} Also at School of Physics and Engineering, Sun Yat-sen University, Guangzhou, China.

^{ah} Also at Institute for Nuclear Research and Nuclear Energy (INRNE) of the Bulgarian Academy of Sciences, Sofia, Bulgaria.

^{ai} Also at Faculty of Physics, M.V. Lomonosov Moscow State University, Moscow, Russia.

^{aj} Also at National Research Nuclear University MEPhI, Moscow, Russia.

^{ak} Also at Department of Physics, Stanford University, Stanford, CA, United States.

^{al} Also at Institute for Particle and Nuclear Physics, Wigner Research Centre for Physics, Budapest, Hungary.

^{am} Also at Flensburg University of Applied Sciences, Flensburg, Germany.

^{an} Also at University of Malaya, Department of Physics, Kuala Lumpur, Malaysia.

^{ao} Also at CPPM, Aix-Marseille Université and CNRS/IN2P3, Marseille, France.

^{ap} Also affiliated with PKU-CHEP.

* Deceased.